

Fock-space diagonalization of the state-dependent pairing Hamiltonian with the Woods-Saxon mean field

H. Molique and J. Dudek

Institut de Recherches Subatomiques, IN₂P₃-CNRS/Université Louis Pasteur, F-67037 Strasbourg Cedex 2, France

(Received 6 May 1997)

A particle-number conserving approach is presented to solve the nuclear mean-field plus pairing Hamiltonian problem with a realistic deformed Woods-Saxon single-particle potential. The method is designed for the state-dependent monopole pairing Hamiltonian $\hat{H}_{\text{pair}} = \sum_{\alpha\beta} G_{\alpha\beta} c_{\alpha}^{\dagger} c_{\alpha}^{\dagger} c_{\beta} c_{\beta}$ with an arbitrary set of matrix elements $G_{\alpha\beta}$. Symmetries of the Hamiltonians on the many-body level are discussed using the language of \mathcal{P} symmetry introduced earlier in the literature and are employed to diagonalize the problem; the only essential approximation used is a many-body (Fock-space) basis cutoff. An optimal basis construction is discussed and the stability of the final result with respect to the basis cutoff is illustrated in details. Extensions of the concept of \mathcal{P} symmetry are introduced and their consequences for an optimal many-body basis cutoff construction are exploited. An algorithm is constructed allowing to solve the pairing problems in the many-body spaces corresponding to $p \sim 40$ particles on $n \sim 80$ levels and for several dozens of lowest lying states with precision $\sim (1-2) \%$ within seconds of the CPU time on a CRAY computer. Among applications, the presence of the low-lying seniority $s=0$ solutions, that are usually poorly described in terms of the standard approximations (BCS, HFB), is discussed and demonstrated to play a role in the interpretation of the spectra of rotating nuclei. [S0556-2813(97)02210-3]

PACS number(s): 21.60.Ev, 21.10.Re, 21.30.Fe, 27.70.+q

I. INTRODUCTION

In the nuclear structure calculations based on the microscopic treatment of the multifermionic systems, the average-field plus pairing Hamiltonian played a central role in the past. Despite visible progress in the nuclear shell-model techniques, the approximations employing either the deformed potentials of the Nilsson or Woods-Saxon type, or those using the Hartree-Fock techniques, turned out to be extremely powerful tools helping us to understand the quantum mechanisms observed, among others, in the high-spin physics or the physics of exotic nuclei.

In order to be realistic, these average-field approximations must be supplemented with residual interactions, the short-range interactions of the pairing type being so far the most commonly used. However, the calculations could only be performed by resorting to approximate methods such as the Bardeen-Cooper-Schrieffer (BCS) or Hartree-Fock-Bogolyubov (HFB) approaches, sometimes in conjunction with the correction terms evaluated within the random-phase approximation (RPA). These approximations have become standard in the nuclear physics literature.

Both BCS and HFB approximations suffer from serious defects, the nonconservation of the number of particles being one of them. Moreover, the precision of these approximations, acceptable for the class of the two quasiparticle excitations, becomes questionable when it comes to four, or higher order excitations. In addition, as mentioned, e.g., by Richardson [1] on the basis of an exactly soluble algorithm for the monopole pairing problem, the two quasiparticle excitations that are interpreted in terms of a standard pair-breaking mechanism are not necessarily the *lowest* excitations of the paired system (see also examples below). Defining the seniority s as the number of unpaired nucleons,

the $s=0$ and $s=2$ excitations are found to compete energetically in the exact solutions, while the $s=0$ exact states correspond within the BCS/HFB type algorithms to four quasiparticles and are predicted to lie far too high in the energy scale. The latter observation implies that an important class of the low-lying excitations in nuclei cannot be described in terms of the standard BCS- or HFB-like theories and this may have further important consequences for our understanding of the nature of excitations, e.g., in exotic nuclei, or some low-spin excitations in rotating nuclei.

Another group of problems with the approximate standard treatment of the pairing Hamiltonian is related to the fact that both the BCS and the HFB approximations break down for an important class of physical situations. The remedy in terms of, e.g., particle number projection techniques complicates the algorithms considerably, yet without helping to approach better the description of the higher-excited part of the spectrum of the pairing Hamiltonian.

Over recent years, some effort has been observed to elaborate algorithms that bypass the Bogolyubov transformation ansatz, and thus are free from problems related to the nonconservation of the particle number. These methods are based on the direct diagonalization of the pairing Hamiltonian in the many-body Fock space.

For instance, in Ref. [2] the pairing Hamiltonian has been diagonalized exactly in the seniority $s=0$ space for an example of 10 fermions distributed over 20 equispaced, doubly degenerate orbitals. It has been found that the number of configurations with the important weights in the lowest-energy solutions is very restricted, only a few lowest-energy configurations contributing significantly. The principle of a truncation of the many-body basis by retaining a certain number of the lowest energy states became an evident working scheme to follow. Furthermore, the superiority of such a

many-body truncation as compared to a single-particle orbital truncation has been demonstrated.

In this context several possibilities have been studied. One of those has been developed in a series of articles [3–6], in which the authors have suggested a method based on a diagonalization of the pairing Hamiltonian in spaces spanned by some energy-truncated ensembles of the many-body wave functions. A discussion of approximate solutions in terms of the truncated many-body (Fock) spaces based on cranked single-particle orbitals can be found in Refs. [7–9]. Extensions to include effective truncations in terms of K (projection of the angular momentum on the elongation axis) are described in Ref. [10]. Another extension using a truncation scheme based on the angular momentum alignment selection is described in Refs. [11,12]. Extensive studies and many applications of the energy truncated many-body basis construction were performed in Refs. [2,13–16]. These applications concern, for example, studies of the K structures of the many-body wave functions, of the yrast-yrare interaction strengths, as well as of the band crossing frequencies.

In the majority of the above mentioned articles, a considerable effort has been attached to a characteristic property of the monopole pairing Hamiltonian: by a certain scaling of the strength constant, the particle number conserving solutions could be brought closer to the BCS solutions and vice versa. Such comparisons are to some extent useful, yet leaving several issues not answered, such as, for example, the quality of the underlying algorithms and their comparison with the exact results, and perhaps most importantly, the stability of the solutions with respect to the basis cutoff.

In the present article, we would like to focus on a study of the particle number conserving algorithms that could be applied for *realistic* nuclear Hamiltonians of essentially two forms. The one related to the nuclear structure problems without collective rotation is

$$\hat{H} = \sum_{\alpha} \varepsilon_{\alpha} (c_{\alpha}^{\dagger} c_{\alpha} + c_{\alpha}^{\dagger} c_{\bar{\alpha}}) - \sum_{\alpha\beta} G_{\alpha\beta} c_{\alpha}^{\dagger} c_{\alpha}^{\dagger} c_{\bar{\alpha}}^{\dagger} c_{\bar{\beta}} c_{\beta}, \quad (1.1)$$

where the creation and annihilation operators for fermions satisfy the usual anti-commutation rules ($\{c_{\alpha}, c_{\beta}^{\dagger}\} = \delta_{\alpha\beta}$ and $\{c_{\alpha}, c_{\beta}\} = 0$); we have also $(c_{\alpha}^{\dagger})^{\dagger} = c_{\alpha}$ and $c_{\alpha}^{\dagger}|0\rangle$ corresponding to states conjugated with respect to $c_{\alpha}^{\dagger}|0\rangle$, e.g., in terms of time-reversal [17] or signature (see below) operations. We will *not* assume that the pairing matrix elements $G_{\alpha\beta}$ must be degenerate to a constant ($G_{\alpha\beta} \sim G$). In other words, most of the conclusions of the present study will remain valid for state-dependent pairing. The second family of Hamiltonians that are of interest here are the so-called cranking Hamiltonians that take the form

$$\hat{H} \rightarrow \hat{H}^{\omega} \equiv \hat{H} - \omega \sum_{\alpha\beta} \langle \alpha | \hat{J}_x | \beta \rangle c_{\alpha}^{\dagger} c_{\beta}. \quad (1.2)$$

In the latter relation the external rotation term (cranking term) describes a rotation of the system about an axis (in this case the \mathcal{O}_x axis).

In the construction of this article we let ourselves be inspired by a previous work [18] where the concept of \mathcal{P} symmetry has been introduced, based on studying relatively small-size systems within an exact diagonalization. Obvi-

ously the question of exploring all possible symmetries of the problem with Hamiltonian matrices of large dimensions plays an important role. Here we would like to discuss both, the aspect of the very existence of the many-body symmetries in the Hamiltonians of interest as well as a possibility of the application of these symmetries in realistic calculations by reducing the sizes of the corresponding Hamiltonian blocks to the minimum.

In the following we present the most general class of \mathcal{P}_1 -symmetric Hamiltonians first. This symmetry is of interest in particular for classifying the rotational states in nuclei as well as in diminishing the sizes of the many-body Hamiltonian blocks, as it will be described in Sec. II. High symmetries of the state-dependent monopole pairing Hamiltonians will be explored, in particular in terms of the seniority (and/or \mathcal{P}_2 symmetry) and \mathcal{P}_1 -quantum number in the deformed nuclear Hamiltonians (1.1) and (1.2). Here also the fact that Hamiltonian (1.1) conserves both the number of particles *and* the number of pairs of particles will explicitly be employed, leading to a tremendous lowering of the sizes of the Hamiltonian blocks. We will introduce a concept of a local weight associated with the many-body (Fock) states and demonstrate how to use this concept to further block-diagonalize analytically the state-dependent monopole-pairing Hamiltonians.

A possibility of practical applications of the above mentioned symmetry considerations requires the tests of stability of the basis cutoff. The illustration of the test of stability allowing to obtain well approximated solutions in the many-body spaces of the Hamiltonian matrices “billion \times billion” or larger by effectively applying only about 1000×1000 matrix diagonalizations, will be presented in Sec. III. We will illustrate the behavior of the obtained solutions using very few configurations, approximating well the results that would require in principle formidably large matrices. As a typical example, the seniority zero eigenvalue problem of a system composed of 32 particles on 64 orbitals would need in principle the use of 601 080 390 configurations, whereas one can obtain stable eigenvalues within a few % accuracy with approximately “a couple of thousand \times a couple of thousand” matrices out of well preselected states. We will also compare in some detail the solutions based on the BCS quasiparticle picture with the model calculations. Section IV will be devoted to applications of the method discussed in this article, in the realistic cases of selected nuclei in the rare-earth mass region. Conclusions and consequences of the results obtained will be discussed in Sec. V.

II. A HIERARCHY OF \mathcal{P} -SYMMETRIC HAMILTONIANS OF DEFORMED NUCLEI

The construction of this chapter follows a hierarchy of symmetries that standard Hamiltonians of a deformed nucleus may obey. Hamiltonian (1.1) is a particular form of a more general structure and we recall briefly a typical chain of Hamiltonian structures that have been widely used in the literature, together with the implied symmetries in the Fock space.

A. Introduction: Nuclear Hamiltonians and dichotomic symmetries

Let us begin with two most commonly exploited dichotomic symmetries of the Hamiltonians of deformed nuclei, the

parity $\hat{\pi}$ and the signature, say, $\hat{R}_x(\pi)$ [a rotation through an angle π about the \mathcal{O}_x axis, $\hat{R}_x(\pi) = \exp(-i\pi\hat{J}_x)$]. The signature symmetry has further going consequences for the many-body structure of the realistic effective Hamiltonians, mainly because pairing Hamiltonians distinguish the interaction scheme that couples the states of opposite signatures (maximum overlap).

Let us introduce a single-particle basis spanned by the eigenstates of a one-body Hamiltonian commuting with a dichotomic symmetry operator, e.g., $\hat{S}(1) \equiv \hat{R}_x(\pi)$ where the argument 1 refers to the one-body representation of the corresponding operators. We then have

$$\hat{H}(1) = \sum_{\alpha\beta} \langle \alpha | \hat{h}(1) | \beta \rangle c_{\alpha}^{\dagger} c_{\beta}; \quad [\hat{S}(1), \hat{h}(1)] = 0, \quad (2.1)$$

and thus we may introduce the states labeled by the eigenvalues of $\hat{S}(1)$. Since the operator in question satisfies $\hat{S}(1)^2 = -1$ in a fermion space, we have a possibility to select a representation in such a way that

$$\begin{aligned} \hat{h}(1) | \alpha s_{\alpha} \rangle &= e_{\alpha s_{\alpha}} | \alpha s_{\alpha} \rangle; \\ \hat{S}(1) | \alpha s_{\alpha} \rangle &= s_{\alpha} | \alpha s_{\alpha} \rangle; \quad s_{\alpha} = \pm i. \end{aligned} \quad (2.2)$$

The corresponding symmetry operator $\hat{S}(2)$ acting in the space of the two particle wave functions can be viewed as a direct product, $\hat{S}(2) = \hat{S}(1) \otimes \hat{S}(1)$.

Within the basis of eigensolutions $| \alpha s_{\alpha} \rangle \equiv | \alpha \pm i \rangle \equiv | \alpha \pm \rangle$ of Hamiltonian $\hat{h}(1)$, one represents any one-body plus two-body Hamiltonian operator in a standard way by

$$\begin{aligned} \hat{H} &= \sum_{\alpha} \varepsilon_{\alpha} (c_{\alpha+}^{\dagger} c_{\alpha+} + c_{\alpha-}^{\dagger} c_{\alpha-}) \\ &+ \frac{1}{2} \sum_{\substack{\alpha\beta \\ \gamma\delta}} \langle \alpha \pm, \beta \pm | \hat{h}(2) | \gamma \pm, \delta \pm \rangle c_{\alpha \pm}^{\dagger} c_{\beta \pm}^{\dagger} c_{\delta \pm} c_{\gamma \pm}. \end{aligned} \quad (2.3)$$

In the above relation there are in fact 16 types of two-body matrix elements, distinguished by the signs (\pm) combined in any possible way. Assuming, as it is often possible, that the two-body operator $\hat{h}(2)$ commutes with $\hat{S}(2)$, $[\hat{h}(2), \hat{S}(2)] = 0$, implies that half of the matrix elements in Eq. (2.3) must vanish. The nonvanishing ones give

$$\hat{H}(2) = \frac{1}{2} \sum_{\substack{\alpha+\beta+ \\ \gamma+\delta+}} \langle \alpha+, \beta+ | \hat{h}(2) | \gamma+, \delta+ \rangle c_{\alpha+}^{\dagger} c_{\beta+}^{\dagger} c_{\delta+} c_{\gamma+} \quad (2.4a)$$

$$+ \frac{1}{2} \sum_{\substack{\alpha+\beta+ \\ \gamma-\delta-}} \langle \alpha+, \beta+ | \hat{h}(2) | \gamma-, \delta- \rangle c_{\alpha+}^{\dagger} c_{\beta+}^{\dagger} c_{\delta-} c_{\gamma-} \quad (2.4b)$$

$$+ \frac{1}{2} \sum_{\substack{\alpha+\beta- \\ \gamma-\delta+}} \langle \alpha+, \beta- | \hat{h}(2) | \gamma-, \delta+ \rangle c_{\alpha+}^{\dagger} c_{\beta-}^{\dagger} c_{\delta+} c_{\gamma-} \quad (2.4c)$$

$$+ \frac{1}{2} \sum_{\substack{\alpha+\beta- \\ \gamma+\delta-}} \langle \alpha+, \beta- | \hat{h}(2) | \gamma+, \delta- \rangle c_{\alpha+}^{\dagger} c_{\beta-}^{\dagger} c_{\delta-} c_{\gamma+} \quad (2.4d)$$

$$+ \frac{1}{2} \sum_{\substack{\alpha-\beta- \\ \gamma+\delta+}} \langle \alpha-, \beta- | \hat{h}(2) | \gamma+, \delta+ \rangle c_{\alpha-}^{\dagger} c_{\beta-}^{\dagger} c_{\delta+} c_{\gamma+} \quad (2.4e)$$

$$+ \frac{1}{2} \sum_{\substack{\alpha-\beta- \\ \gamma-\delta-}} \langle \alpha-, \beta- | \hat{h}(2) | \gamma-, \delta- \rangle c_{\alpha-}^{\dagger} c_{\beta-}^{\dagger} c_{\delta-} c_{\gamma-} \quad (2.4f)$$

$$+ \frac{1}{2} \sum_{\substack{\alpha-\beta+ \\ \gamma-\delta+}} \langle \alpha-, \beta+ | \hat{h}(2) | \gamma-, \delta+ \rangle c_{\alpha-}^{\dagger} c_{\beta+}^{\dagger} c_{\delta+} c_{\gamma-} \quad (2.4g)$$

$$+ \frac{1}{2} \sum_{\substack{\alpha-\beta+ \\ \gamma+\delta-}} \langle \alpha-, \beta+ | \hat{h}(2) | \gamma+, \delta- \rangle c_{\alpha-}^{\dagger} c_{\beta+}^{\dagger} c_{\delta-} c_{\gamma+}. \quad (2.4h)$$

The many-body image of the above Hamiltonian has a two sub-block structure, the two sub-blocks corresponding to the opposite signatures of the total many-body wave functions: ± 1 or $\pm i$. Without further limiting assumptions related to the structure of the nuclear Hamiltonian of a deformed nucleus, no additional simplification is evident. (A standard one due to the Hermitean form of the operators and/or time reversal properties are considered obvious and are employed below in diagonalizations of the Hamiltonians studied here.)

B. \mathcal{P}_1 symmetry and unitary groups

We proceed now to narrow the generality of the form of $\hat{H}(2)$ and to explore the implied symmetries. An important next class of slightly less general Hamiltonians is obtained in Eq. (2.4), the terms (2.4b) and (2.4e) are assumed to be zero. Thus by setting

$$\langle \alpha+, \beta+ | \hat{h}(2) | \gamma-, \delta- \rangle = 0 \quad (2.5a)$$

and

$$\langle \alpha-, \beta- | \hat{h}(2) | \gamma+, \delta+ \rangle = 0, \quad (2.5b)$$

we obtain an interesting family of Hamiltonians that after Ref. [18] will be further on referred to as \mathcal{P} symmetric. There are a few good reasons to be interested in \mathcal{P} -symmetric Hamiltonians in the nuclear physics context. First, the standard nuclear pairing Hamiltonians belong to such a family as a subclass, and thus by studying \mathcal{P} symmetry one obtains some rather unexplored properties of pairing in the many-body spaces (see below). Secondly, \mathcal{P}_1 symmetry, which will

be introduced later in this section, remains a valid symmetry of the one-dimensional cranking Hamiltonians studied very often in the literature.

Below we will give only a short account of the original formulation of the \mathcal{P} symmetry that uses the concept of unitary groups [18]. Next, however, we will extend this concept introducing a hierarchy of \mathcal{P} -type symmetries without making an explicit use of the group theory formalism.

To prepare the discussion of the following section, let us divide the full ensemble of the single-particle states into two subsets denoted as above by $\{|\alpha+\rangle\}$; $\alpha=1,2,\dots,N_+$ and $\{|\alpha-\rangle\}$; $\alpha=1,2,\dots,N_-$ such that the following direct-sum relation is satisfied:

$$\{|\alpha\rangle\}=\{|\alpha+\rangle\}\oplus\{|\alpha-\rangle\}; \quad N_++N_-=n, \quad (2.6)$$

n denoting the total number of the single-particle levels. The numbers N_+ and N_- may, but do not need to be equal. For simplicity we will assume that the number n is even, and that $N_+=N_-=N$. The physical criteria for introducing the above subdivision into two ensembles may vary, but there are at least three following cases which are encountered most often in nuclear structure applications: (a) The two ensembles correspond to the opposite time reversal properties, e.g., $|\alpha+\rangle=\hat{T}|\alpha-\rangle$; (b) the two ensembles differ in terms of the *signature* symmetry so that $\hat{\mathcal{R}}_x(1)|\alpha_\pm\rangle=r_\pm|\alpha_\pm\rangle$, where the signature quantum number $r_\pm=\pm i$; (c) the two ensembles differ in terms of the simplex quantum number [simplex operator, say, $\hat{\mathcal{S}}_x(1)\equiv\hat{\pi}\exp(-i\pi\hat{J}_x)$, $\hat{\pi}$ being the parity operator], so that $\hat{\mathcal{S}}_x|\alpha_\pm\rangle=s_\pm|\alpha_\pm\rangle$ where the simplex quantum number $s_\pm=\pm i$.

In the Hamiltonians of the form

$$\hat{H}=\sum_{\alpha\beta}^n\langle\alpha|\hat{h}(1)|\beta\rangle c_{\alpha}^{\dagger}c_{\beta}+\frac{1}{2}\sum_{\alpha\beta\gamma\delta}^n\langle\alpha\beta|\hat{h}(2)|\gamma\delta\rangle c_{\alpha}^{\dagger}c_{\beta}^{\dagger}c_{\delta}c_{\gamma} \quad (2.7)$$

[where $\hat{h}(1)$ may contain a one-dimensional cranking term] we may trivially anticommute the operators $c_{\beta}^{\dagger}c_{\delta}$, leading to a modified expression that can be cast into the form

$$\hat{H}=\sum_{\alpha\beta}^n\langle\alpha|\hat{h}'(1)|\beta\rangle\hat{n}_{\alpha\beta}-\frac{1}{2}\sum_{\alpha\beta\gamma\delta}^n\langle\alpha\beta|\hat{h}(2)|\gamma\delta\rangle\hat{n}_{\alpha\delta}\hat{n}_{\beta\gamma}, \quad (2.8)$$

where

$$\langle\alpha|\hat{h}'(1)|\beta\rangle=\langle\alpha|\hat{h}(1)|\beta\rangle+\frac{1}{2}\sum_{\gamma}^n\langle\alpha\gamma|\hat{h}(2)|\beta\gamma\rangle, \quad (2.9)$$

and where

$$\hat{n}_{\alpha\beta}\equiv c_{\alpha}^{\dagger}c_{\beta}. \quad (2.10)$$

As is well known

$$[\hat{n}_{\alpha\beta},\hat{n}_{\gamma\delta}]=\delta_{\beta\gamma}\hat{n}_{\alpha\delta}-\delta_{\alpha\delta}\hat{n}_{\gamma\beta}, \quad \alpha,\beta,\gamma,\delta=1,2,\dots,n, \quad (2.11)$$

a relation coinciding with that of the unitary-group generators.

Similar to Ref. [18], we may identify $\hat{n}_{\alpha\beta}$ with the generators $\hat{G}_{\alpha\beta}$ of the unitary group in n dimensions and write down the corresponding Hamiltonian in the many-body space

$$\hat{H}=\sum_{\alpha\beta}^n\langle\alpha|\hat{h}'(1)|\beta\rangle\hat{G}_{\alpha\beta}-\frac{1}{2}\sum_{\alpha\beta\gamma\delta}^n\langle\alpha\beta|\hat{h}(2)|\gamma\delta\rangle\hat{G}_{\alpha\delta}\hat{G}_{\beta\gamma}, \quad (2.12)$$

where the n^2 operators $\hat{G}_{\alpha\beta}$ represent matrices of dimension $\dim(n,p)\equiv\binom{p}{n}$ each.

We can also introduce the Casimir operator

$$\hat{C}=\sum_{\alpha}^n\hat{n}_{\alpha\alpha}=\sum_{\alpha}^n\hat{G}_{\alpha\alpha}. \quad (2.13)$$

So far all the expressions (2.7)–(2.13) are general and standard. Assuming that Hamiltonian (2.12) commutes with $\hat{\mathcal{S}}$ and recalling that we are particularly interested in the case of vanishing of the matrix elements in Eqs. (2.5a)–(2.5b) we proceed by rewriting first the form of the Casimir operator:

$$\begin{aligned} \hat{C} &= \sum_{\alpha+}^{N_+} \hat{n}_{\alpha+\alpha+} + \sum_{\alpha-}^{N_-} \hat{n}_{\alpha-\alpha-} \\ &= \underbrace{\sum_{\alpha+}^{N_+} c_{\alpha+}^{\dagger}c_{\alpha+}}_{\hat{\mathcal{N}}_1^+} + \underbrace{\sum_{\alpha-}^{N_-} c_{\alpha-}^{\dagger}c_{\alpha-}}_{\hat{\mathcal{N}}_1^-} = \hat{\mathcal{N}}_1^+ + \hat{\mathcal{N}}_1^-. \end{aligned} \quad (2.14)$$

It is straightforward to show that Hamiltonian (2.12) after limiting its generality as just specified does not only commute with \hat{C} but also with $\hat{\mathcal{N}}_1^+$ and $\hat{\mathcal{N}}_1^-$ separately, and that $\hat{\mathcal{N}}_1^+$ and $\hat{\mathcal{N}}_1^-$ commute with \hat{C} and among themselves. Consequently, both the particle-number operator $\hat{\mathcal{N}}_1^+ + \hat{\mathcal{N}}_1^-$ and the new operator of the *difference* $\hat{\mathcal{N}}_1^+ - \hat{\mathcal{N}}_1^-$, arbitrarily denoted $\hat{\mathcal{P}}_1$ in Ref. [18] (where the term ‘‘ \mathcal{P} symmetry’’ comes from)

$$\hat{\mathcal{N}}_1 \equiv \hat{\mathcal{N}}_1^+ + \hat{\mathcal{N}}_1^-$$

and

$$\hat{\mathcal{P}}_1 \equiv \hat{\mathcal{N}}_1^+ - \hat{\mathcal{N}}_1^- \quad (2.15)$$

commute with the Hamiltonian, and we arrive at a possibility of bringing the Hamiltonian in question into a block-diagonal form, each block labeled by the \mathcal{P}_1 -quantum number.

Observe that all the above operators have been written in the many-body (Fock) space. Independently of a possible formal derivation of the spectrum of the $\hat{\mathcal{P}}_1$ operator, one can easily deduce such a spectrum. Recalling that [cf. Eqs. (2.14) and (2.15)] $\hat{\mathcal{P}}_1$ is a difference between the operators representing the number of particles occupying single-particle states of symmetry + and the number of particles occupying the states of symmetry –, we see immediately that the possible eigenvalues of \mathcal{P}_1 are

TABLE I. Table illustrating the block structure of a $\hat{\mathcal{P}}_1$ -symmetric Hamiltonian for an example of $p=16$ particles on $n=32$ single-particle levels. The table indicates the possible values of the \mathcal{P}_1 -quantum number, and the corresponding dimensions of the Hamiltonian sub-blocks. The total number of many-body configurations spanning the complete space is $C_{16}^{32}=601\,080\,390$.

\mathcal{P}_1 value	Dimension
0	165 636 900
± 2	130 873 600
± 4	64 128 064
± 6	19 079 424
± 8	3 312 400
± 10	313 600
± 12	14 400
± 14	256
± 16	1

$$\mathcal{P}_1 = p, p-2, p-4, \dots, -p \quad (2.16)$$

for a system of p particles on n levels with $p \leq n/2$, and

$$\mathcal{P}_1 = (n-p), (n-p-2), (n-p-4), \dots, -(n-p) \quad (2.17)$$

for a system for which $n/2 \leq p \leq n$. (From now on, p and n will be assumed to be even, for simplicity.)

Hamiltonian (2.12) splits therefore into $(p+1)$ sub-blocks in the case of Eq. (2.16) and in $(n-p)+1$ sub-blocks in the case of Eq. (2.17). Table I illustrates the corresponding dimensionalities for an ‘‘academic test’’ system of $p=16$ particles on $n=32$ levels. It is easily seen that the dimension of a given block characterized by the quantum number \mathcal{P}_1 is given by

$$\dim(\mathcal{P}_1) = C_{(p+\mathcal{P}_1)/2}^N C_{(p-\mathcal{P}_1)/2}^N. \quad (2.18)$$

Recall that the condition for the validity of the above results is that the Casimir operator can be split into two terms as in Eq. (2.14), i.e., that $[\hat{h}(1), \hat{S}(1)]=0$ and $[\hat{h}(2), \hat{S}(2)]=0$, and excluding the matrix elements (2.5a) and (2.5b) as announced earlier. Consequently, the most general form of a $\hat{\mathcal{P}}_1$ -symmetry-conserving Hamiltonian is the one composed of only six terms in Eq. (2.4); those in Eqs. (2.4b)–(2.4e) are excluded.

C. \mathcal{P}_1 symmetry as a concept independent of the unitary group considerations

Although the first mention of \mathcal{P} symmetry and possible profits for the Hamiltonians of the deformed nuclei, Ref. [18], involved the unitary group language together with the use of the Casimir operators, etc., an important aspect of the block-diagonalization of the many-body Hamiltonians can be obtained rather easily using directly the properties of the Fock-space vectors.

The mechanism called \mathcal{P} symmetry [18] can be summarized as follows. Suppose that a Hamiltonian \hat{H} commutes with two operators, say $\hat{\mathcal{N}}^+$ and $\hat{\mathcal{N}}^-$ that characterize a certain set of configurations in the Fock space and

$[\hat{\mathcal{N}}^+, \hat{\mathcal{N}}^-]=0$. The corresponding many-body states can be labeled with $(\mathcal{N}^+, \mathcal{N}^-)$. That form, however, may not be the most general neither the most convenient to express the corresponding block-diagonalization procedure of the Hamiltonian. There exists Hamiltonians of interest in nuclear and solid state physics whose form allows us to find the relation $[\hat{H}, \hat{\mathcal{P}}_1 = \hat{\mathcal{N}}^+ - \hat{\mathcal{N}}^-]=0$ while $[\hat{H}, \hat{\mathcal{N}}^+ + \hat{\mathcal{N}}^-] \neq 0$. To stress this point that illustrates certain advantages of the formulation in terms of ‘‘ $\hat{\mathcal{P}} = \hat{\mathcal{N}}^+ - \hat{\mathcal{N}}^-$ ’’ language let us refer to an important class of the Hamiltonians discussed in Appendix A.

D. Generalized pairing Hamiltonians as a particular case of a \mathcal{P}_1 -symmetric operator

If in Eq. (2.4) only the four terms (2.4c), (2.4d), (2.4g), and (2.4h) are retained, the two-body Hamiltonian may be written in the form

$$\begin{aligned} \hat{H}_{gp}(2) = & \frac{1}{2} \sum_{\substack{\alpha+\beta- \\ \gamma-\delta+}} \langle \alpha+\beta- | \widetilde{\hat{h}(2)} | \gamma-\delta+ \rangle c_{\alpha+}^{\dagger} c_{\beta-}^{\dagger} c_{\delta+} c_{\gamma-} \\ & + \frac{1}{2} \sum_{\substack{\alpha-\beta+ \\ \gamma-\delta+}} \langle \alpha-\beta+ | \widetilde{\hat{h}(2)} | \gamma-\delta+ \rangle \\ & \times c_{\alpha-}^{\dagger} c_{\beta+}^{\dagger} c_{\delta+} c_{\gamma-} \end{aligned} \quad (2.19)$$

[where we have introduced the antisymmetrized matrix elements $\langle \alpha\beta | \widetilde{\hat{h}(2)} | \gamma\delta \rangle \equiv \langle \alpha\beta | \hat{h}(2) | \gamma\delta \rangle - \langle \alpha\beta | \hat{h}(2) | \delta\gamma \rangle$]. In this case the corresponding operator obviously still obeys the \hat{S} symmetry and the $\hat{\mathcal{P}}_1$ symmetry. Operators of that general form are referred to as generalized pairing Hamiltonians since the only interaction allowed here is the scattering of *pairs* of nucleons of the opposite \hat{S} symmetry ($s_{\alpha} = \pm i$, $s_{\beta} = \mp i$).

Those Hamiltonians preserve their $\hat{\mathcal{P}}_1$ symmetry also in the case of the cranking version with the \hat{S} symmetry preserving one-body term of Eq. (1.2)

$$\hat{H} \rightarrow \hat{H}^{\omega} = \hat{H}(1) + \hat{H}_{gp}(2) - \omega_x \hat{J}_x \quad (2.20)$$

since the operator

$$\begin{aligned} \hat{J}_x = & \sum_{\alpha+} \sum_{\beta+} \langle \alpha+ | \hat{J}_x | \beta+ \rangle c_{\alpha+}^{\dagger} c_{\beta+} \\ & + \sum_{\alpha-} \sum_{\beta-} \langle \alpha- | \hat{J}_x | \beta- \rangle c_{\alpha-}^{\dagger} c_{\beta-} \end{aligned} \quad (2.21)$$

also commutes with both $\hat{\mathcal{N}}_1^+$ and $\hat{\mathcal{N}}_1^-$.

E. State-dependent monopole-pairing Hamiltonian as a particular case of a \mathcal{P}_1 -symmetric operator

By narrowing the allowed choice of the coupling scheme in Eq. (2.4) to only those nucleonic pairs that occupy the mutually time-reversed (or mutually signature inversed) orbitals, we obtain a general form of what is called a monopole-pairing Hamiltonian:

$$\hat{H}_{\text{mp}}(2) = \frac{1}{2} \sum_{\alpha\beta} \langle \alpha^\pm, \alpha^\mp | \hat{h}(2) | \beta^\pm, \beta^\mp \rangle c_{\alpha^\pm}^\dagger c_{\alpha^\mp}^\dagger c_{\beta^\mp} c_{\beta^\pm}, \quad (2.22)$$

the summation in Eq. (2.22) containing formally four groups of terms with the s symmetries

$$\begin{aligned} & (+-, +-), (+-, -+), (-+, +-), \\ & \text{and } (-+, -+). \end{aligned} \quad (2.23)$$

The state-dependent monopole-pairing Hamiltonian obeys the \mathcal{P}_1 symmetry as a particular case of more general \mathcal{P}_1 -symmetric structures discussed above, and consequently its matrix structure in the many-body space takes a block-diagonal form labeled with the \mathcal{P}_1 quantum numbers. The \mathcal{P}_1 quantum numbers may then take the values listed in Eqs. (2.16) and (2.17).

F. \mathcal{P}_1 symmetry and the seniority scheme; \mathcal{P}_2 symmetry

In this section we are going to combine the \mathcal{P}_1 -symmetry scheme of nuclear Hamiltonians composed of the average field and state-dependent monopole-pairing terms and the seniority structure.

Let us focus first on the static (i.e., no rotation) case. We assume that the average field term has already been diagonalized so that the Hamiltonian takes the form (1.1)

$$\hat{H} = \sum_{\alpha} \varepsilon_{\alpha} (c_{\alpha}^{\dagger} c_{\alpha} + c_{\alpha}^{\dagger} c_{\bar{\alpha}}) - \sum_{\alpha\beta} G_{\alpha\beta} c_{\alpha}^{\dagger} c_{\alpha}^{\dagger} c_{\bar{\beta}} c_{\beta}. \quad (2.24)$$

Let us introduce many-body states expressed through the occupation labels

$$[(p_{\alpha_1}, p_{\bar{\alpha}_1}), (p_{\alpha_2}, p_{\bar{\alpha}_2}) \cdots (p_{\alpha_N}, p_{\bar{\alpha}_N})]. \quad (2.25)$$

Those states are defined in the following way:

$$\begin{aligned} |(p_{\alpha_1}, p_{\bar{\alpha}_1}) \cdots (p_{\alpha_N}, p_{\bar{\alpha}_N})\rangle &\equiv (c_{\alpha_1}^{\dagger})^{p_{\alpha_1}} (c_{\bar{\alpha}_1}^{\dagger})^{p_{\bar{\alpha}_1}} (c_{\alpha_2}^{\dagger})^{p_{\alpha_2}} \\ & (c_{\bar{\alpha}_2}^{\dagger})^{p_{\bar{\alpha}_2}} \cdots (c_{\alpha_N}^{\dagger})^{p_{\alpha_N}} (c_{\bar{\alpha}_N}^{\dagger})^{p_{\bar{\alpha}_N}} |0\rangle. \end{aligned} \quad (2.26)$$

Symbol (2.26) represents a totally antisymmetric state in the Fock space if

$$P_{(\alpha_i \text{ or } \bar{\alpha}_i)} = \begin{cases} 1 & \text{for the state } \alpha_i(\bar{\alpha}_i) \text{ occupied} \\ 0 & \text{otherwise;} \end{cases} \quad (2.27a)$$

and

$$\sum_{i=1}^N (p_{\alpha_i} + p_{\bar{\alpha}_i}) = p, \quad (2.27b)$$

where p denotes the number of particles and N the number of available pairwise-conjugate single-particle orbitals.

Within the above notation, the seniority equal to two states are characterized by occupation vectors in which strictly two pairs of indices $(p_{\alpha_i}, p_{\bar{\alpha}_i})$ satisfy one of the following equalities:

$$s=2: \quad (p_{\alpha_i}, p_{\bar{\alpha}_i}) = (0,1) \quad \text{or} \quad (p_{\alpha_i}, p_{\bar{\alpha}_i}) = (1,0). \quad (2.28)$$

Seniority $s=4$ states are characterized by occupation vectors in which strictly four pairs of indices are correlated through

$$\begin{aligned} & [(p_{\alpha_i}, p_{\bar{\alpha}_i}); (p_{\alpha_j}, p_{\bar{\alpha}_j}); (p_{\alpha_k}, p_{\bar{\alpha}_k}); (p_{\alpha_l}, p_{\bar{\alpha}_l})] \\ & \Rightarrow [(1,0) \text{ or } (0,1); (1,0) \text{ or } (0,1); \\ & (1,0) \text{ or } (0,1); (1,0) \text{ or } (0,1)], \end{aligned} \quad (2.29)$$

etc. Let us now introduce, in analogy to the operators $\hat{\mathcal{N}}_1^+$ and $\hat{\mathcal{N}}_1^-$ (cf. Sec. II B), the following two operators:

$$\hat{\mathcal{N}}_2^+ \equiv \sum_{i=1}^N c_{\alpha_i}^{\dagger} c_{\alpha_i}^{\dagger} c_{\bar{\alpha}_i} c_{\alpha_i} \quad (2.30)$$

and

$$\hat{\mathcal{N}}_2^- \equiv \sum_{i=1}^N (1 - c_{\alpha_i}^{\dagger} c_{\alpha_i}^{\dagger} c_{\bar{\alpha}_i} c_{\alpha_i}). \quad (2.31)$$

They both commute, and in addition they also commute with Hamiltonian (2.24). It is easy to show that the action of operator (2.30) on states (2.26) gives the number of *paired* couples, while the action of the operator (2.31) gives the number of conjugate orbitals not occupied by a pair of particles.

Continuing in analogy to the discussion of the \mathcal{P}_1 symmetry, where the symmetry of single-particle states together with the properties of the one-body Hamiltonian-related operators $\hat{\mathcal{N}}_1^+$ and $\hat{\mathcal{N}}_1^-$ has been exploited, we may now define two auxiliary many-body operators related to two-body terms in the Hamiltonian

$$\hat{\mathcal{N}}_2 \equiv \hat{\mathcal{N}}_2^+ + \hat{\mathcal{N}}_2^- \quad (2.32)$$

and

$$\hat{\mathcal{P}}_2 \equiv \hat{\mathcal{N}}_2^+ - \hat{\mathcal{N}}_2^-. \quad (2.33)$$

Since all of the above operators commute among themselves as well as with the Hamiltonian [Eq. (2.24)], we have

$$[\hat{\mathcal{N}}_2, \hat{H}] = 0$$

and

$$[\hat{\mathcal{P}}_2, \hat{H}] = 0. \quad (2.34)$$

The action of the operator $\hat{\mathcal{P}}_2$ on states (2.26) gives

$$\hat{\mathcal{P}}_2 |(p_{\alpha_1}, p_{\bar{\alpha}_1}) \cdots (p_{\alpha_N}, p_{\bar{\alpha}_N})\rangle = \mathcal{P}_2 |(p_{\alpha_1}, p_{\bar{\alpha}_1}) \cdots (p_{\alpha_N}, p_{\bar{\alpha}_N})\rangle, \quad (2.35)$$

where \mathcal{P}_2 may take any of the following values:

$$\mathcal{P}_2 = p - N, p - 2 - N, \dots, -N, \quad (2.36a)$$

for $p \leq n/2$, and

$$\mathcal{P}_2 = p - N, p - 2 - N, \dots, 2(p - N) - N \quad (2.36b)$$

if $n/2 \leq p \leq n$. The states with \mathcal{P}_2 and $\mathcal{P}'_2 \neq \mathcal{P}_2$ do not couple through the Hamiltonian (2.24) and consequently the corresponding Hamiltonian-matrix structure becomes block diagonal in terms of the \mathcal{P}_2 quantum number as well.

Let us observe that the operators (2.32), (2.33) [or (2.30), (2.31)] commute with the $\hat{\mathcal{P}}_1$ operator introduced in Sec. II B, and consequently we may write, in addition to Eq. (2.35),

$$\hat{\mathcal{P}}_1 |(p_{\alpha_1}, p_{\bar{\alpha}_1}) \cdots (p_{\alpha_N}, p_{\bar{\alpha}_N})\rangle = \mathcal{P}_1 |(p_{\alpha_1}, p_{\bar{\alpha}_1}) \cdots (p_{\alpha_N}, p_{\bar{\alpha}_N})\rangle, \quad (2.37)$$

where in the present context \mathcal{P}_1 can take the following values:

$$\mathcal{P}_1 = -s, -s + 2, -s + 4, \dots, +s. \quad (2.38)$$

Each block of a given \mathcal{P}_2 quantum number can be divided into $(s + 1)$ sub-blocks of the different \mathcal{P}_1 quantum numbers given in Eq. (2.38). Of course, the conservation of parity would allow for further splitting of the above structure.

In the static case (no rotation), both the \mathcal{P}_1 and the \mathcal{P}_2 symmetries can be applied simultaneously; in such a case the many-body solutions can be labeled by $|(p_{\alpha_1}, p_{\bar{\alpha}_1}) \cdots (p_{\alpha_N}, p_{\bar{\alpha}_N})\rangle_{\mathcal{P}_1, \mathcal{P}_2, \nu}$, where ν denotes all possible quantum numbers other than \mathcal{P}_1 and \mathcal{P}_2 . In the case of a one-dimensional rotation, the seniority scheme (or \mathcal{P}_2 scheme) does not, in general, offer any simplification in terms of block-diagonal structures whereas the \mathcal{P}_1 symmetry does remain an exact symmetry of the corresponding Hamiltonian.

An example of the block structure of the discussed Hamiltonian for the system of $p = 16$ particles on $n = 32$ levels is given in Table II. At this stage it will be instructive to consider the dimensions of the sub-blocks of given \mathcal{P}_2 (or seniority s) and \mathcal{P}_1 quantum numbers. It is straightforward to show that these dimensions are given by

$$\begin{aligned} \dim(\mathcal{P}_2, \mathcal{P}_1) &= C_{(p-N-\mathcal{P}_2+\mathcal{P}_1)/2}^N C_{(p-N-\mathcal{P}_2-\mathcal{P}_1)/2}^{N-(p-N-\mathcal{P}_2+\mathcal{P}_1)/2} C_{(N+\mathcal{P}_2)/2}^{2N-p+\mathcal{P}_2}. \end{aligned} \quad (2.39)$$

From formula (2.39), the full dimensions of the blocks of given \mathcal{P}_2 (or seniority s) quantum numbers are therefore

$$\dim(\mathcal{P}_2) = \sum_{\mathcal{P}_1 = -s}^{\mathcal{P}_1 = +s} \dim(\mathcal{P}_2, \mathcal{P}_1), \quad (2.40)$$

the summation being such that \mathcal{P}_1 take the values (2.38).

G. Further block diagonalization of Hamiltonians with state-dependent pairing; \mathcal{P}_{12} symmetry

Here we would like to discuss yet another important block-diagonalization of the Hamiltonians in question. Pursuing the scheme of \mathcal{P}_1 and \mathcal{P}_2 symmetries, let us consider the following construction. First we will identify a given many-body state (2.26) with its occupation representation

TABLE II. Table illustrating the reduction of the \mathcal{P}_2 /seniority blocks into sub-blocks of different \mathcal{P}_1 -quantum number. The system considered is the same as the one illustrated in Table I. The third and the last columns indicate the dimensions of the \mathcal{P}_2 /seniority blocks and those of the \mathcal{P}_1 sub-blocks, respectively. Recall that the \mathcal{P}_2 and seniority quantum numbers are related through $\mathcal{P}_2 = 2\mathcal{N}_2^+ - N$, \mathcal{N}_2^+ denoting the number of single-particle states occupied pairwise and N the number of available pairwise-conjugate states. Note that for the particular example chosen here one has simply $\mathcal{P}_2 = -s$.

Seniority	\mathcal{P}_2	Dimension	\mathcal{P}_1 values	Dimension
0	0	12 870	0	12 870
2	-2	1 647 360	0	823 680
			± 2	411 840
4	-4	26 906 880	0	10 090 080
			± 2	6 726 720
			± 4	1 681 680
			± 6	2 018 016
6	-6	129 153 024	0	40 360 320
			± 2	30 270 240
			± 4	12 108 096
			± 6	2 018 016
			± 8	900 900
			± 10	160 160
8	-8	230 630 400	0	63 063 000
			± 2	50 450 400
			± 4	25 225 200
			± 6	7 207 200
			± 8	900 900
			± 10	160 160
			± 12	10 920
			± 14	240
10	-10	164 003 840	0	40 360 320
			± 2	33 633 600
			± 4	19 219 200
			± 6	7 207 200
			± 8	1 601 600
			± 10	160 160
			± 12	10 920
			± 14	240
			± 16	16
			± 18	1
12	-12	44 728 320	0	10 090 080
			± 2	8 648 640
			± 4	5 405 400
			± 6	2 402 400
			± 8	720 720
			± 10	131 040
			± 12	10 920
			± 14	240
			± 16	16
			± 18	1
			± 20	1
			14	-14
± 2	720 720			
± 4	480 480			
± 6	240 240			
± 8	87 360			
± 10	21 840			
± 12	3360			
± 14	240			
± 16	16			
± 18	1			
± 20	1			
± 22	1			
± 24	1			
16	-16	65 536		
			± 2	11 440
			± 4	8008
			± 6	4368
			± 8	1820
			± 10	560
			± 12	120
			± 14	16
			± 16	1
			± 18	1
			± 20	1
			± 22	1
			± 24	1
			± 26	1
			± 28	1

(2.25) or, equivalently, with its binary-number representation. This is always possible because of the condition (2.27a). We associate with each position of a label α_i or $\bar{\alpha}_i$ in a symbol (2.25) a weight factor defined with the help of an index $\mu_i \equiv 2i - 2$ as follows:

$$\alpha_i \rightarrow 2^{\mu_i}; \quad \bar{\alpha}_i \rightarrow 2^{\mu_i+1}. \quad (2.41)$$

According to this construction, each position in the symbol (2.25) carries the weight (2.41) if the corresponding single-particle state is occupied, or zero otherwise. We introduce, in an analogy to the construction in Secs. II B and II F, the operators

$$\hat{\mathcal{N}}_{12}^+ \equiv \sum_{i=1}^N (2^{\mu_i} c_{\alpha_i}^\dagger c_{\alpha_i} + 2^{\mu_i+1} c_{\alpha_i}^\dagger c_{\bar{\alpha}_i}) \quad (2.42)$$

and

$$\hat{\mathcal{N}}_{12}^- \equiv \sum_{i=1}^N (2^{\mu_i} + 2^{\mu_i+1}) c_{\alpha_i}^\dagger c_{\bar{\alpha}_i} c_{\bar{\alpha}_i}^\dagger c_{\alpha_i}. \quad (2.43)$$

With the help of these two operators we introduce a new \mathcal{P} -type operator

$$\hat{\mathcal{P}}_{12} \equiv \hat{\mathcal{N}}_{12}^+ - \hat{\mathcal{N}}_{12}^-. \quad (2.44)$$

The indices 12 refer to the fact that $\hat{\mathcal{P}}_{12}$ operator is expressed in terms of ‘‘one-body’’ and ‘‘two-body’’ representations simultaneously. It is now straightforward to show that $\hat{\mathcal{P}}_{12}$ commutes with the Hamiltonian (2.24) as well as with the operators $\hat{\mathcal{P}}_1$ and $\hat{\mathcal{P}}_2$ introduced earlier. Observe also that $\hat{\mathcal{N}}_{12}^+$ and $\hat{\mathcal{N}}_{12}^-$ are linearly independent of the $\hat{\mathcal{N}}^+$ - and $\hat{\mathcal{N}}^-$ -type operators introduced above, and therefore they can be used to generate an independent symmetry as well. The meaning of the operators (2.42)–(2.43) is as follows. The many-body states (2.25) are eigenvectors of the operator $\hat{\mathcal{N}}_{12}^+$, the eigenvalues being simply the sum of the weights of the occupied single-nucleon states corresponding uniquely to the binary representation of these states. This number will be called the *total weight* of the many-body configuration, and the numbers 2^{μ_i} (and 2^{μ_i+1}) are the *partial weights* of the single-particle states α_i (and $\bar{\alpha}_i$). (The weight concept introduced here differs from the one used, e.g., in Ref. [19].) The action of $\hat{\mathcal{N}}_{12}^-$ on these states gives the sum of the powers of 2 for the corresponding doubly degenerate orbitals if they are occupied, and zero otherwise. Let us also introduce a concept of a class of many-body states; all states that have the same particle-hole structure i.e., strictly the same particle states occupied and strictly the same hole states empty but differ in terms of the excitations in pairs form a common class. It is easily seen that, by acting with $\hat{\mathcal{P}}_{12}$ on a state (2.25), one obtains an eigenvalue that characterizes uniquely (i.e. through a one-to-one correspondence) a class of states. With this construction, the states first classified according to their \mathcal{P}_1 and \mathcal{P}_2 quantum numbers can be grouped further into subclasses labeled with the help of \mathcal{P}_{12} .

A similar subdivision into blocks obtained formally in a slightly different manner is exploited in Ref. [20]. An ex-

TABLE III. Illustration of a reduction of the \mathcal{P}_2 Hamiltonian blocks into sub-blocks of different \mathcal{P}_{12} -quantum number. The system considered is the same as the system relative to Table I.

Seniority	\mathcal{P}_2	Full dimension	Number of sub-blocks	Dim. of sub-block
0	0	12 870	1	12 870
2	-2	1 647 360	480	3432
4	-4	26 906 880	29 120	924
6	-6	129 153 024	512 512	252
8	-8	230 630 400	3 294 720	70
10	-10	164 003 840	8 200 192	20
12	-12	44 728 320	7 454 720	6
14	-14	3 932 160	1 966 080	2
16	-16	65 536	65 536	1

ample of the corresponding $(\mathcal{P}_2, \mathcal{P}_{12})$ structure is given in Table III for the case of 16 particles on 32 levels. As it becomes clear from the table, the increasing-seniority states (decreasing \mathcal{P}_2 states) form the Hamiltonian blocks of decreasing size. However the *number* of such blocks increases rapidly for the lowest values of seniority. A formula for the dimensions of the different sub-blocks can be found in Ref. [20]. Of course, it can be checked that the sum of the dimensions of these \mathcal{P}_{12} sub-blocks with the same \mathcal{P}_2 values must lead to the dimensions obtained previously in Eq. (2.40) with the use of the \mathcal{P}_1 substructure.

The above scheme is obviously very advantageous. We may decide *a priori* which class of states are of particular interest for an application. For a given \mathcal{P}_2 (or seniority) quantum number the corresponding matrices to diagonalize have the same dimension, often orders of magnitude smaller than that related to the traditional seniority scheme.

In the present paper we aim at the effective calculations for the heaviest nuclei as well as for lighter ones. As it has been demonstrated by numerous calculations employing the pairing interactions, the spaces of *single-particle states* correspond roughly to an energy window ($\lambda_F - 5$ MeV, $\lambda_F + 5$ MeV) where λ_F denotes the Fermi level. Such an energy window contains usually $p \sim (30$ to $40)$ particles on $n \sim (60$ to $80)$ levels. Spaces of this size produce, even after applying the $(\mathcal{P}_1, \mathcal{P}_2, \mathcal{P}_{12})$ reduction, the many-body matrices that are still relatively large. For $p = 32$ particles on $n = 64$ levels we obtain in analogy to the first few entries in Table III: $\mathcal{P}_2 = 0 \rightarrow \dim_{\text{block}} = 601\,080\,390$, $\mathcal{P}_2 = -2 \rightarrow \dim_{\text{subblocks}} = 155\,117\,520$, etc. These blocks are the most important since the corresponding solutions are among the lowest in energy. Since our goal is to construct a rapid algorithm, one that can be used to generate, e.g., the nuclear potential energy surfaces with pairing (similar to those of, e.g., Ref. [21], the latter obtained without taking the pairing into account), we see that a direct diagonalization is not advantageous. For that reason we replace such a scheme by a Lanczos approach and proceed to develop a many-body basis construction optimized in such a way that an efficient cutoff will become possible. To convince ourselves that the average field plus pairing Hamiltonians allow for such solutions (and anticipating a detailed discussion of the next section), we present in Table IV a stability test obtained for the $s = \mathcal{P}_2 = 0$ solutions with the Lanczos method and our basis optimization dis-

TABLE IV. Evolution of the first four $s=\mathcal{P}_2=0$ excitation energies (in MeV) in function of the many-body basis configurations for a system of $p=32$ particles on $n=64$ equispaced (1 MeV) doubly degenerate levels. The pairing constant is $G=0.345$ MeV. The many-body basis contains the ground state, all the $16\times 16=256$ (one-pair states), and the number of two-pair states is increased in the consecutive diagonalizations. The total number of many-body basis states N_T is indicated in each column. The last column indicates the first two exact excitations obtained with the Richardson method [1].

State No.	$N_T=2\ 050$	$N_T=3\ 243$	$N_T=4\ 225$	$N_T=4\ 763$	$N_T=5\ 920$	$N_T=6\ 529$	$N_T=7\ 145$	$N_T=7\ 769$	Exact
1	2.961	2.973	2.992	3.003	3.027	3.039	3.051	3.063	3.107
2	4.871	4.814	4.799	4.796	4.797	4.800	4.805	4.810	4.900
3	5.008	4.970	4.966	4.968	4.977	4.983	4.990	4.998	
4	6.919	6.840	6.813	6.805	6.815	6.801	6.900	6.903	

cussed in detail later compared to the exact results of Richardson for $p=32$ particles on $n=64$ levels (for the exact results, only the first two eigenvalues are indicated). These examples demonstrate that already at the dimensions of the order of a couple of thousand very precise results are obtained. Storing only the nonzero matrix elements and using the Lanczos technique one can perform this kind of calculation on a personal computer; more efficient machines take a minute to some seconds of CPU time.

A great advantage in this context is that the transition energies (the differences among the calculated levels) stabilize much faster with respect to the basis cutoff as compared to the absolute values of eigenenergies. This allows us to accelerate the algorithms even further.

The above mentioned block-diagonalization scheme remains valid also in the case of an interesting (but so far not well explored in the literature) class of Hamiltonians for rotating nuclei

$$\begin{aligned} \hat{H}^\omega = & \sum_{\alpha} \varepsilon_{\alpha}^{\omega} c_{\alpha}^{\dagger}(\omega) c_{\alpha}(\omega) + \sum_{\alpha} \varepsilon_{\alpha}^{\omega} c_{\alpha}^{\dagger}(\omega) c_{\bar{\alpha}}(\omega) \\ & - \sum_{\alpha\beta} G_{\alpha\beta; \bar{\alpha}\bar{\beta}}(\omega) c_{\alpha}^{\dagger}(\omega) c_{\bar{\alpha}}^{\dagger}(\omega) c_{\bar{\beta}}(\omega) c_{\beta}(\omega), \end{aligned} \quad (2.45)$$

where $|\alpha, \omega\rangle \equiv c_{\alpha}^{\dagger}(\omega)|0\rangle$ denotes a single-particle Routhian of a given signature symmetry and $|\bar{\alpha}, \omega\rangle$ its signature partner, while $G_{\alpha\beta; \bar{\alpha}\bar{\beta}}(\omega)$ represents the rotation-dependent matrix elements, e.g., in the form of an overlap between the corresponding signature partners. A study of the Hamiltonians of this form is in progress and will be reported elsewhere.

Except for the Hamiltonians of the type (2.45), the above scheme does not hold if a rotation term is included in the Hamiltonian, because the cranking term in the case of collective rotation couples different sub-blocks of \mathcal{P}_2 and \mathcal{P}_{12} symmetries.

III. MANY-BODY BASIS CONSTRUCTION FOR REALISTIC HAMILTONIANS

We begin by discussing a technique of handling the many-body basis; we then proceed to illustrate the applied constructions in the tests of stability with respect to the many-body cutoff.

A. Principles of the basis construction and of the cutoff

The many-body basis to be used consists of a finite ensemble of fully antisymmetric many-particle configurations constructed out of n single-nucleon states occupied by $p \leq n$ particles, Eq. (2.26).

In the first step the ground state configuration is constructed. This state corresponds by definition to the configuration in which all the lowest-lying single-particle orbitals are occupied pairwise. In the static case these are usually the Kramers-degenerate states [17]. In the second step we construct $s=0$ excited configurations by promoting *pairs* of particles to originally inoccupied levels. Next we construct $s=2$ excited configurations by creating one-particle–one-hole ($1p-1h$) many-body basis states. Each new particle-hole state is supplemented with its pair excitation ensemble (obtained as in the second step above) leading to a class of its own that does not couple through Hamiltonian (2.24) with another class of states built on a different $1p-1h$ state. Our interest is to apply that scheme for as large spaces as possible: we feel that $n \sim 80$, $p \sim 40$ offers sufficiently rich space for realistic calculations in heavy nuclei. The configurations corresponding to particle-hole excitations lower than a given energy cutoff are retained and the stability of the final results with respect to the basis cutoff is tested with the exact ones obtained through the Richardson method. Then the same selection is performed for “two-particle–two-hole” ($2p-2h$), “three-particle–three-hole” ($3p-3h$) states, etc. One-pair states turn out to be the most important since they directly couple to the ground state via the two-body interaction; this is illustrated below.

B. An example of a full diagonalization

Let us consider an “academic” case of $p=10$ particles on $n=20$ levels for which the diagonalization is done easily without any basis cutoff. The model used here has been studied often in the literature, see, e.g., Ref. [2].

In order to illustrate the role of the “one-pair,” “two-pair,” “three-pair” . . . $s=0$ states, we give in Table V the structure of the first 20 ($s=0$) eigenstates for this system. The single-particle levels are composed of equispaced (1 MeV) doubly degenerate orbitals, the first orbital chosen arbitrarily at the energy of 1 MeV. The pairing strength parameter is taken to be $G=0.5$ MeV.

The dimension of the full $s=0$ space is 252. It is clearly seen from the table that the most important contributions come from the ground state and the “one-pair” and “two-

TABLE V. Structure of the exact first twenty ($s=0$) solutions of a system composed of 10 particles on 20 equispaced (1 MeV) doubly degenerate levels. The pairing strength is $G=0.5$ MeV. The percentages indicate the sum of the amplitude squares of the different basis states in the eigensolutions.

No.	Energy (MeV)	% GS	% one pair	% two pair	% three pair	% four, five pair
1	0.000	60.14	35.49	4.22	0.15	0.00
2	2.806	27.81	63.80	8.09	0.30	0.00
3	4.716	6.39	82.12	10.98	0.51	0.00
4	4.716	0.00	94.45	5.46	0.09	0.00
5	6.662	1.99	85.66	11.83	0.52	0.00
6	6.662	0.07	89.18	10.52	0.23	0.00
7	7.149	0.19	93.94	5.66	0.21	0.00
8	8.635	0.88	85.30	13.24	0.57	0.01
9	8.635	0.02	86.83	12.76	0.39	0.00
10	8.888	0.85	14.65	80.71	3.78	0.01
11	9.178	0.15	91.35	8.15	0.35	0.00
12	9.178	0.00	91.48	8.33	0.20	0.00
13	10.637	0.42	84.66	14.29	0.63	0.00
14	10.637	0.00	85.38	14.09	0.53	0.00
15	11.128	0.38	13.05	83.09	3.49	0.00
16	11.128	0.01	11.90	86.32	1.77	0.00
17	11.170	0.04	86.00	13.59	0.37	0.00
18	11.199	0.08	90.22	9.30	0.40	0.00
19	11.199	0.00	90.28	9.39	0.32	0.01
20	12.958	0.18	5.86	89.49	4.47	0.00

pair” states. The states of more complicated structure (four and five pairs excited) have almost no contribution in as high as ~ 10 MeV above the ground state. Let us remark that the number of “five-pair” states is only one in this particular example and that the number of “four-pair” configurations is not very large; there are as many “four-pair” as “one-pair” configurations. However, we will see that also for much richer spaces ($n > 20$, $p > 10$) the role of the high-order pair-excitation configurations is very limited, resembling to this academic case (cf. the following section).

C. Basis cutoff and convergence study on larger model spaces for $s=0$ solutions

The stability of the final results with respect to the basis cutoff is a primordial aspect. As the next case let us consider once again the example of a model space composed of $p=16$ particles distributed over $n=32$ levels representing a single-particle spectrum of the same type as in the previous section. We have again set $G=0.5$ MeV, so that this example corresponds to a realistic situation in light nuclei leading to a gap between the lowest eigensolution and the first excited solution of 3.715 MeV.

The dimension of the full $s=0$ many-body space is in this case $N_{\text{mb}}=12\ 870$. The largest seniority zero basis we have considered with our cutoff procedure was composed of the ground state (always taken into account), the 64 ($=8 \times 8$) all existing “one-pair,” 428 “two-pair” (out of 784 possibilities), and 400 “three-pair” (out of 3136) states (reference cutoff). We have varied the number of the “one-pair,” “two-pair” and “three-pair” $s=0$ basis states separately in order to study the convergence properties. The results are given in Fig. 1, where the absolute energies are plotted. From these results we can see that the eigenvalues are most sensi-

tive to the selection of the “one-pair” states, especially for the low-lying solutions. The coupling between the “one-pair” and the “two-pair” states on the one hand and between the “two-pair” and the “three-pair” states on the other hand influences more the higher-excited solutions in the spectrum.

This result is intuitively understandable if we recall that, e.g., the “three-pair” states are of high excitation energies (the lowest excitation being equal to 18 MeV in this case) and thus they mix much less with the low-energy solutions. This mechanism should of course be even more pronounced if we consider for instance “four-pair” states, and calculations (not displayed) show that this is indeed the case.

An important indication here is that applying the only energetic cutoff criteria as studied in Ref. [3], is not sufficient to ensure a high quality of the many-body basis. A similar point has also been remarked by other authors [22]. More precisely, in the discussed example, one has to take into account at least *all* the “one-pair” states and some “two-pair” states to obtain a good-precision description of the lowest $s=0$ solutions. The influence of the “one-pair” states on the final result stability shows a characteristic feature (see Fig. 1): the energies of excited states converge very regularly when the number of these basis states increases. Since the curves in question are nearly parallel, the stability of the diagonalization results for the *transition energies* is better than that of the absolute eigenvalues.

This typical behavior does not depend very much on the dimensions of the *single-particle* space used, as illustrated in Fig. 2 for the spectrum obtained by diagonalizing the same Hamiltonian but for $p=40$ particles distributed over $n=80$ equispaced doublets separated by 0.3 MeV; the pairing strength here is $G=0.114$ MeV. We see from this

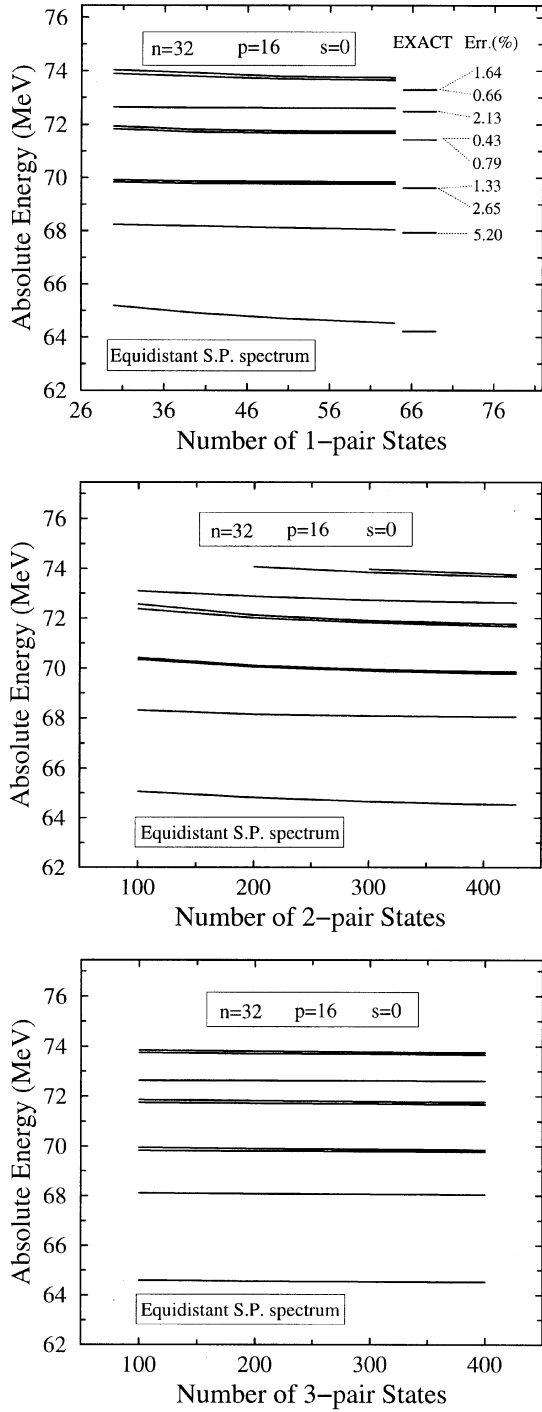


FIG. 1. Stability of the seniority zero eigenvalues in function of the number of “one-pair,” “two-pair,” and “three-pair” states. The calculations correspond to a model system containing 16 particles distributed over 32 equispaced doubly degenerate orbitals (the first double orbital lies arbitrarily at 1 MeV, and the level spacing is 1 MeV). The pairing strength is $G=0.5$ MeV. The largest many-body space considered here (also called “reference cutoff”) is composed of the ground state, 64 “one-pair,” 428 “two-pair,” and 400 “three-pair” states. The right-hand side spectrum in the first plot corresponds to the exact solutions; for each eigenvalue, the relative difference (absolute values) between the calculated excitations (normalized to the ground state) and the exact ones are indicated in this case.

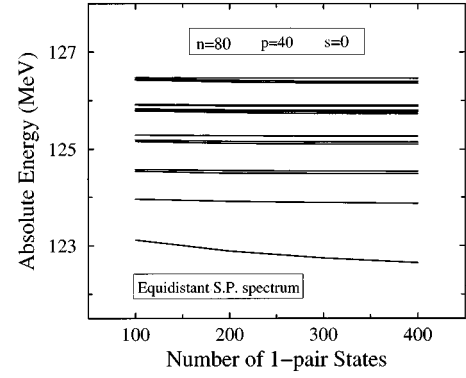


FIG. 2. Similar to the first spectrum in Fig. 1, but for $p=40$ particles distributed over $n=80$ doubly degenerate orbitals separated by 0.3 MeV. Here the pairing strength is $G=0.114$ MeV. The largest many-body space (reference cut-off) is composed now of the ground state, 400 “one-pair,” 300 “two-pair,” 150 “three-pair” states, and 50 “four-pair” states.

figure that the lowest lying eigenvalue is the most sensitive with respect to an increase in number of “one-pair” states, whereas the excited states stabilize again in fact very rapidly, similarly to the previously discussed case of much smaller dimensionalities.

In order to demonstrate the degree of precision one can obtain with the above described basis construction, let us present an example for $p=32$ particles on $n=64$ levels taken from Table IV. The dimension of the full $s=0$ space is in this case $N_{mb}=601\,080\,390$. A diagonalization (using the Lanczos technique) in a space composed of the ground state, the total number of “one-pair” states (256 configurations) and 6272 “two-pair” states gives for the first and second excitation energies the values 3.039 and 4.800 MeV; the exact results are 3.107 and 4.900 MeV. Therefore the first two excitation energies are calculated with a precision of 2.19 and 2.04 %, respectively, whereas the number of basis states represent approximately 0.001% of the full space.

The way of constructing an ensemble of many-body basis configurations that are adapted to the specificities of the pairing interaction studied, together with the explicit use of the concept of \mathcal{P} symmetry is referred to, in the following, as PSY-MB (\mathcal{P} symmetry and many-body) method.

D. PSY-MB method vs BCS approximation

1. The $s=0$ solutions

In this section we shall analyze the main differences among the solutions obtained by using the PSY-MB and the BCS methods, as compared to the exact solutions. In this example we use once more the model space composed of 16 fermions distributed over 32 equispaced (1 MeV) double orbitals; the constant pairing interaction is again used with $G=0.5$ MeV. We will consider here only the solutions corresponding to seniority zero states as demanding the most important numerical effort.

The PSY-MB basis used is composed of the reference cutoff introduced in Sec. III C. The exact solution is obtained with the Richardson method (see Refs. [1,23,24]): the corresponding eigenenergies are those relative to the right-hand side part of the first spectrum calculated in Fig. 1, top.

TABLE VI. Absolute value of the lowest lying eigensolution obtained with different methods. The PNC solution is described in Ref. [3]. The system studied is the same as described by the spectra in Fig. 1.

	E_{GS} (MeV)	$ E_{GS} - E_{GS, \text{exact}} $ (MeV)
Exact	64.492	0
BCS	66.411	1.919
PNC	66.130	1.638
PSY-MB	64.799	0.307

We can see clearly from Fig. 1 that the Fock-space diagonalization offers excellent results although only a minute part of the full basis is retained. In fact, we have used in our calculation only 893 states, whereas the full spectrum contains $C_8^{16} = 16!/8!8! = 12\,870$ configurations.

In Table VI we indicate the absolute value of the energy of the lowest eigenstate obtained within several methods. In this Table, PNC (particle number conserving method) denotes a simplified approach to the problem, described in Ref. [3], where the configurations are selected according to only simple energy cutoff criteria. One can check easily that in the PNC calculations whose results are taken from Ref. [3], the many-body basis is composed of the ground state, 36 “one-pair” and 30 “two-pair” states, i.e., all the configurations with the excitation energies lower than 16 MeV. We include the results obtained with this smaller basis to point out the discrepancies that may appear if this basis is too restricted. Although the absolute value of the lowest eigensolution has no physical interest, it should be used as a measure of the accuracy of the method itself. The results point out that the ground state solution given by the BCS approximation is rather inaccurate. In order to confirm this point we have plotted in Fig. 3 the occupation probabilities of the single-particle orbitals in the ground solution, and it is seen that the

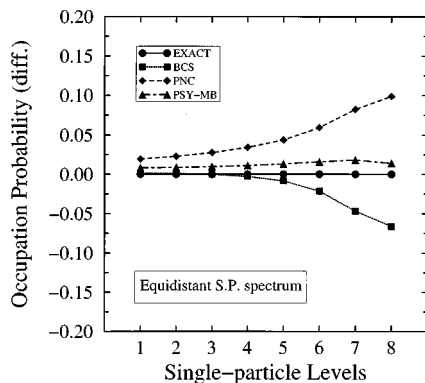


FIG. 3. Occupation probabilities, relative to the exact solution, of the single-particle orbitals in the lowest lying eigensolution of the physical system illustrated in Fig. 1. The plot shows the differences between the results obtained with various approaches and the exact results. In this figure, PNC denotes the results obtained by using the same basis as in Ref. [3]. Note that the figure illustrates only the occupation probabilities of the “hole” states (i.e., the states below the Fermi surface); the occupation probabilities of the particle states can be deduced immediately by symmetry considerations, and are therefore not indicated.

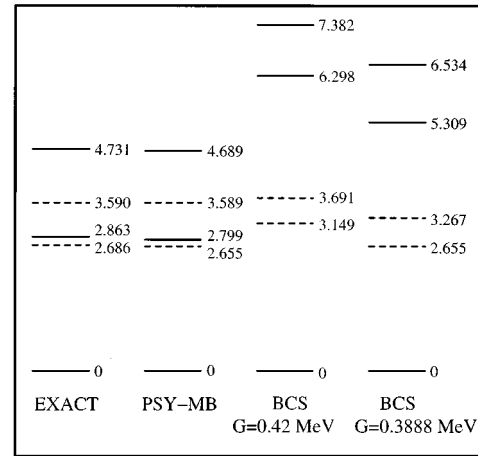


FIG. 4. Excitation spectra obtained for the same system as that relative to Fig. 1. For the three first spectra the pairing constant is $G = 0.42$ MeV. The excited states with seniority zero are plotted as full lines, the solutions with seniority $s = 2$ corresponding to the dashed lines in the plot. For the PSY-MB method, the latter states are obtained by diagonalizing the many-body Hamiltonian involving $3p-3h$ configurations generated in classes (see text) built on a different $1p-1h$ “parent” state. One can note that the obtained eigenvalues are highly degenerate. (As an example: one can construct four $1p-1h$ configurations with the same lowest energies. As the corresponding doublets of orbitals are blocked in the same way, this leads to a fourfold degenerate many-body solution). The basis used for the seniority $s = 0$ states corresponds to the reference cutoff in Fig. 1. We have plotted the spectrum obtained by two and four quasiparticle excitations in the BCS formalism. The spectrum on the right-hand side of the figure corresponds to a BCS calculation with the pairing interaction strength adjusted to the value $G = 0.3888$ MeV. See text for more details.

PSY-MB method gives significantly better agreement with the exact solution.

The authors of Ref. [3] argue that the PNC approximation leads to too strong pairing effects. We believe that the solutions obtained with the PNC approach offer a quality comparable to that of the BCS results, because the used PNC basis is too small (similar point was raised in Ref. [22]). In addition it should be mentioned that in Ref. [3] the comparisons with the quasiparticle excitations were made by using a readjusted value of the BCS pairing strength so that the direct comparison with the exact treatment seems to be additionally biased.

2. The $s \neq 0$ solutions

We would like to focus on the states with seniority $s \neq 0$. We consider here the same system as in the previous section, but with the pairing strength somewhat modified ($G = 0.42$ MeV). This value corresponds exactly to one of the values used by Richardson [1] who has compared the BCS solutions to the exact ones in several model spaces. In Fig. 4 we have plotted the excitation spectrum obtained by diagonalizing the Hamiltonian with the PSY-MB method, in comparison with the exact spectrum. For completeness, we have illustrated the seniority zero states (solid lines) as well as the states with seniority $s = 2$ (dashed lines) on the same plot. As we can see from the figure, the basis selection proposed here works very

well, whereas we have only used $1p-1h$ states and $3p-3h$ states. The latter are grouped in different “families” (classes), each family being generated out of a given $1p-1h$ state and corresponding to the Hamiltonian block dimension $N_d=49$. The reduction of the dimensions can be easily seen as follows. For each member of the same “family,” the four single-particle levels participating in the $1p-1h$ excitation will be blocked. Therefore, there are $7 \times 7 = 49$ possibilities to create $3p-3h$ states by exciting one pair of particles in the remaining space. One obtains very accurate solutions within such a strongly limited space, because blocking of some levels leads to gaps in the single-particle spectrum thus weakening the pairing. For comparison, Table III shows that by not using the discussed scheme one would need to perform the diagonalization of matrices $3\,432 \times 3\,432$ (see $\mathcal{P}_2 = -2$ sub-blocks).

3. Quasiparticle excitations and $s=0$ and $s=2$ solutions

To complete our very limited comparison of the PSY-MB and BCS method results with the exact solutions, let us present the description of the excited states in terms of the BCS quasiparticles (QP’s).

We consider here the same physical system as the one of the previous section; the results of the calculations are also illustrated in Fig. 4.

We will follow here the usual interpretation, see, e.g., [1], according to which the states corresponding to two QP excitations are related, at the vanishing pairing limit, to the one particle one hole excitations; these states correspond to the dashed lines in Fig. 4 and should be compared to the solutions of seniority $s=2$. The four QP states are represented by solid lines and should be compared to the $s=0$ excitations.

We can read from Fig. 4 that the BCS description of excited states in terms of quasiparticles differs considerably from the exact solutions.

It has been argued by several authors that one could possibly improve the description in the BCS approach by readjusting the pairing constant. Following this kind of an approach, we adjusted the BCS pairing strength to locate the first 2 QP state at the value obtained by the PSY-MB result (viz. 2.655 MeV). The adjusted value is $G=0.3888$ MeV. The corresponding new spectrum is plotted on the right-hand side of Fig. 4. Although this spectrum is more “compressed,” the results remain unsatisfactory.

One of the most important drawbacks of the solutions constructed on the basis of quasiparticle excitations is that the excited states corresponding to four QP lie systematically higher in energy as compared to those constructed with two quasiparticles. This point seems to be essential in a correct interpretation of the experimental spectra in terms of pairing. As can be seen on the basis of the exact calculations with the Richardson method, or with the use of the PSY-MB method, it is possible that the $s=0$ solutions (corresponding structurally to four QP excitations in the BCS formalism) may become lower in energy than the two QP-type solutions which is an evident conflict since the four QP BCS excitations lie markedly higher than the two QP excitations.

In order to illustrate this specific point, we have reported in Fig. 5 the calculated many-body spectra for the neutrons in the nuclei ^{160}Yb , ^{170}Yb , and ^{174}Yb . The figure illustrates the spectra obtained for different pairing strengths (see next

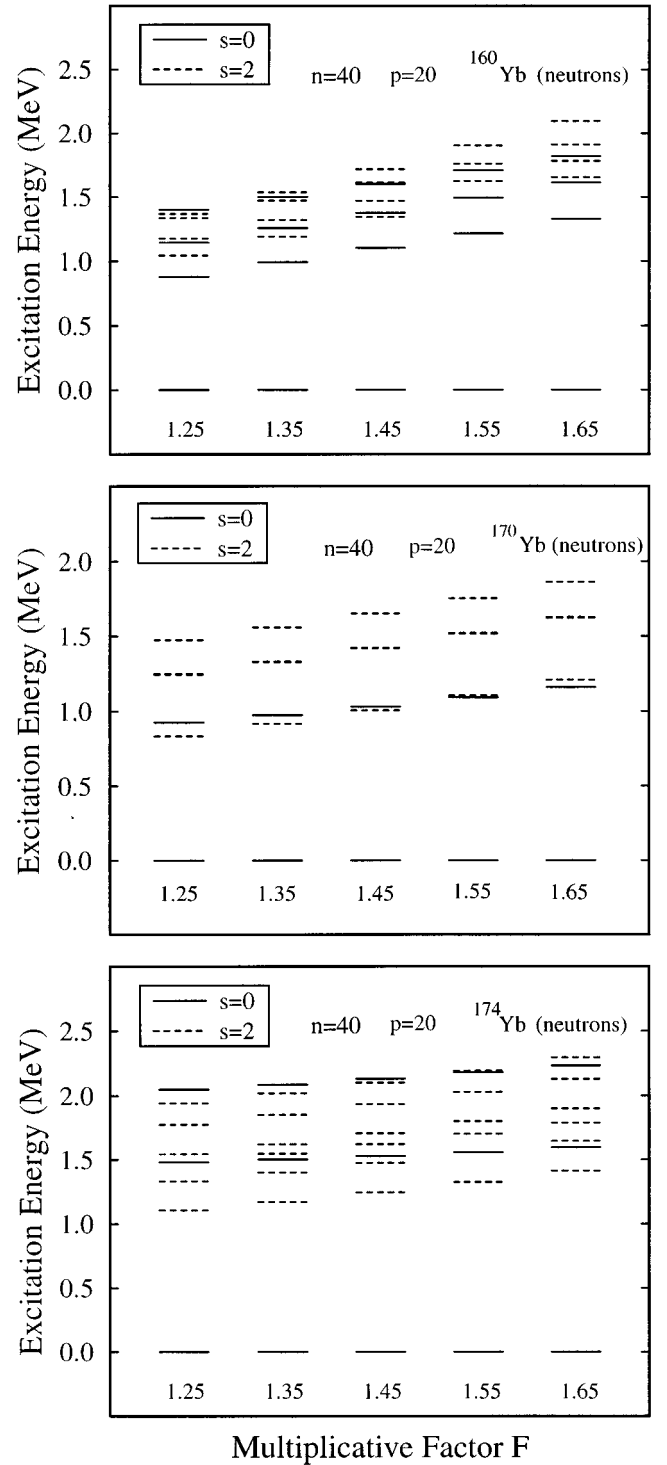


FIG. 5. Evolution of the calculated many-body spectra in function of the pairing strength parameter. The system studied is composed of $p=20$ neutrons distributed over $n=40$ single-particle Woods-Saxon orbitals located around the Fermi level for the nuclei ^{160}Yb , ^{170}Yb , and ^{174}Yb . Deformation of the potential, $\alpha_{20}=0.294$, $\alpha_{40}=-0.017$.

section). To complete the comparison, we have plotted in Fig. 6 the used single-particle Woods-Saxon spectra for each nucleus, indicating in each case the position of the Fermi energy λ . It appears clearly that the order of the $s=0$ and $s=2$ lowest solutions depends on the level density and the

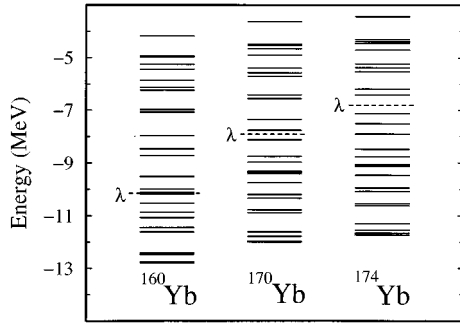


FIG. 6. Figure illustrating the neutron level density around the Fermi surface, in the Woods-Saxon single-particle spectrum, for the three nuclei studied in Fig. 5.

pairing, which is intuitively clear; what is less evident is that for the physically reasonable strength constants and realistic single-particle spectra the lowest $s=0$ solutions compete with the lowest $s=2$ solutions: if the pairing strength becomes larger, the seniority zero solutions may become lower in energy than the seniority two states.

E. A state-dependent model interaction: Gaussian dependence in $G_{\alpha\beta}$

Constant pairing-strength interaction is not a very good approximation to the physical situation in nuclei. In fact, within such an approach a transition amplitude (pairing matrix element) for a pair of states say, 1 MeV distant and, say, 25 MeV distant, are the same and equal to G in contrast to what one would expect for realistic many-body systems. We would like to illustrate a simple alternative, interesting from the PSY-MB point of view, by considering an interaction where the pairing strength is given by a Gaussian-type function

$$G_{\alpha\beta} = A e^{-B(e_{\alpha} - e_{\beta})^2}, \quad (3.1)$$

where e_{α} and e_{β} represent single-particle (Woods-Saxon) energies of the states α and β . The parameters A and B are adjusted in such a way that the location of the first excited eigensolution lies approximately at the same energy as for the constant pairing case. Of course, there is some freedom in adjusting those parameters, allowing to control in a phenomenological manner the interaction among the states that differ more and more in energy. Expression (3.1) allows us to model in a schematic way the interactions between the couples of single-particle states (α, β) that are closest in energy. The scattering between particles occupying such states will be favored, whereas scatterings between particles in states whose energies differ importantly will be reduced.

We have illustrated in Fig. 7 the convergence behavior of the calculated spectrum in the case of this model interaction. The most interesting feature consists of the fact that the convergence is, as one might expect, more rapid than in the case of the constant pairing (see also next section). It seems that the lowest eigenvalue converges rapidly, even if only a few one pair states are used in the calculations. For the Fock-space diagonalization approach such a model dependence seems extremely encouraging because of both, the physical advantages mentioned above and the convergence properties.

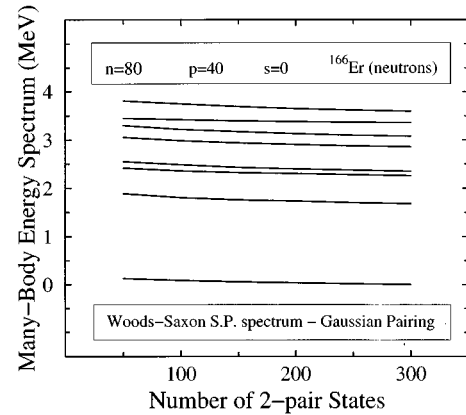
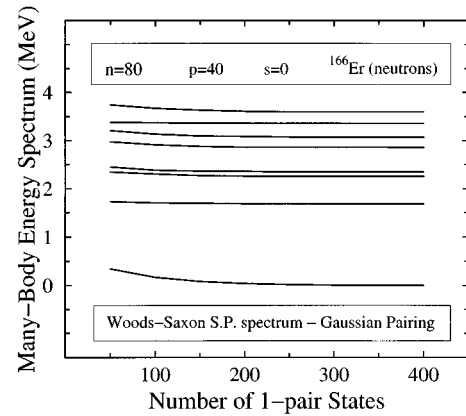


FIG. 7. The top Figure is similar to Fig. 2, but for a Gaussian-type pairing and the Woods-Saxon neutron spectrum of ^{166}Er . The figure also illustrates the behavior of the solutions with respect to the number of “two-pair” states in the many-body basis, bottom. The reference cutoff basis is composed here of the ground state, 400 “one-pair,” 300 “two-pair,” and 150 “three-pair” states. (For plotting convenience, the spectra are shifted by an arbitrary constant.)

However, an optimal parametrization of the $G_{\alpha\beta}$ matrix to the Woods-Saxon spectra and systematic comparison with experiment need still to be studied.

F. The $s=0$ and $s \neq 0$ solutions for a realistic single-particle Woods-Saxon spectrum

So far we have shown that the procedure used in the PSY-MB method for selecting the many-body basis configurations is effective, offering a fast stabilization of the final result with respect to the many-body basis cutoff. We would like to extend the discussion further to realistic situations. For this purpose we plot in Fig. 8 the calculated energies of the many-body problem obtained for an example of a single-particle neutron Woods-Saxon spectrum, for the nucleus ^{166}Er . Again a constant pairing interaction has been used here.

The figure shows that for a realistic case one obtains easily a stabilization of the final $s=0$ result as well. In particular, it appears that the convergence of the solutions is improved when the two-pair states are considered. One is also interested in the particle-hole configurations with seniority $s=2$ or higher seniority values.

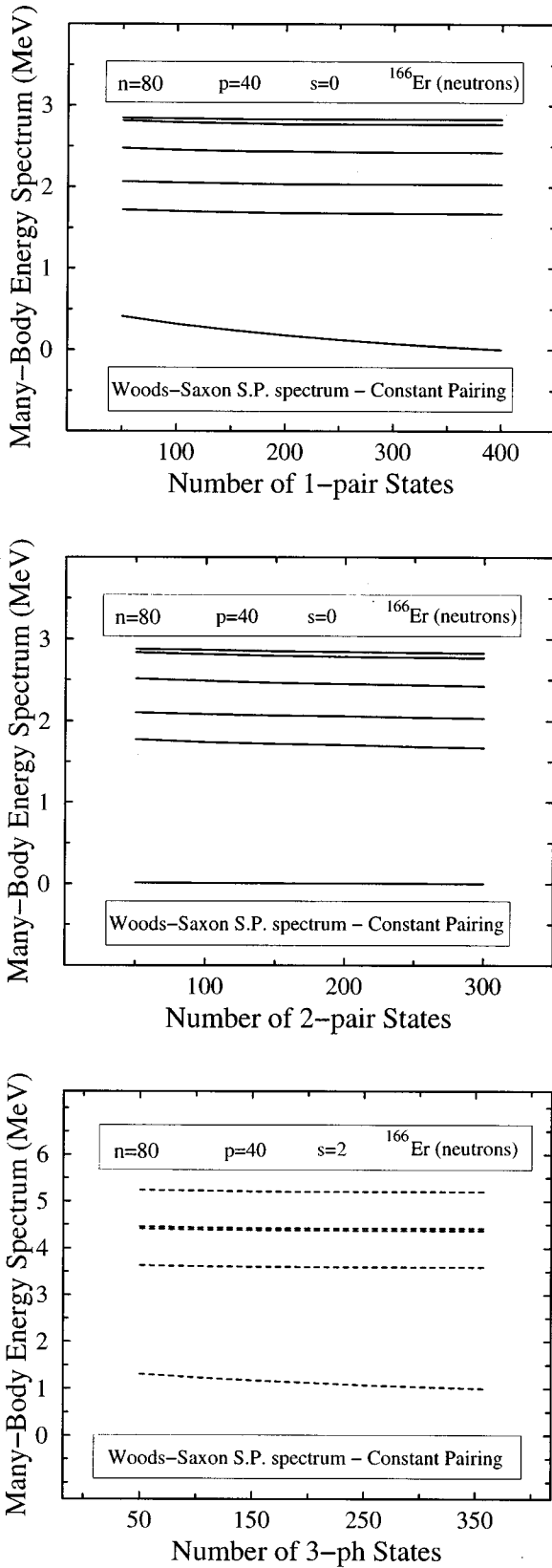


FIG. 8. Similar to Fig. 7, but for the constant pairing interaction. The reference cutoff for $s=0$ (top and middle) is the same as in Fig. 7. Here is also indicated the behavior of the $s=2$ solutions with respect to the number of $3p-3h$ states in the many-body basis, bottom. These $3p-3h$ correspond to the class (see text) constructed on a common $1p-1h$ parent configuration.

Here again, we have let ourselves be guided by the fact that the pairing Hamiltonian annihilates and creates *pairs* of particles. We have proven by a direct calculation that the PSY-MB way of proceeding is much more efficient than that using a construction of any set of $3p-3h$ states and applying an energetic cutoff criteria alone, for the studies of higher-excited solutions.

We illustrate a characteristic behavior of the eigenvalues in function of the number of ($s=2$) $3p-3h$ configurations in the basis for a realistic spectrum in Fig. 8, bottom, where we have plotted the corresponding PSY-MB spectrum for the case of the neutron single-particle Woods-Saxon levels for ^{166}Er . These calculations are performed using a family of $3p-3h$ states built on a chosen common $1p-1h$ parent configuration (in this case a $1p-1h$ with lowest excitation energy). The convergence properties in the ($s=2$) case are even better than in the ($s=0$) case. This is because the blocked levels are located near the Fermi level; as mentioned previously, their blocking creates effectively an increased gap in the spectrum, leading to a reduced effect of the pairing Hamiltonian, and thus intuitively explaining an accelerated convergence of the solutions. We can note in relation to this specific example that the number of levels below and above the Fermi level are in both cases equal to 40. It is therefore straightforward to realize that the total number of the ($s=2$) $3p-3h$ states one can construct with the above scheme is equal to $19 \times 19 = 361$, the value appearing on the right-hand side in the corresponding spectrum of Fig. 8, bottom. Let us remark that formally these calculations resemble to an $s=0$ calculation in an auxiliary configuration space spanned by $(p-2)$ particles on $(n-4)$ levels. The gap introduced is of advantage, making the effects of possible higher-order pair excitations significantly smaller.

IV. SOME REALISTIC CALCULATIONS; \mathcal{P} SYMMETRY AND ROTATION

We would like to illustrate the use of the optimized basis selection method in realistic calculations for selected nuclei in the rare-earth mass region. The results presented have been obtained by choosing as the valence space the one spanned by $p=20$ particles distributed over $n=40$ single-particle Woods-Saxon orbitals located around the Fermi level. After having performed the stability tests like those discussed in detail in the preceding section, we have retained the many-body basis composed of the following 901 configurations: (a) The ground-state configuration, (b) 100 (one pair) states ($=10 \times 10$, all possible states), (c) 100 (two pairs) states, (d) 400 ($1p-1h$) states ($=20 \times 20$, all possible states), (e) 150 ($2p-2h$) states and, (f) 150 ($3p-3h$) states. For the one-body cranking term, the one pair and $1p-1h$ states are of major importance. The quadrupole and hexadecapole deformations have been taken from Ref. [25]. We have also made use of the parity conservation to reduce further the sizes of the Hamiltonian blocks. This is important from a numerical point of view, because the dimensions of the matrices to be diagonalized diminish roughly by a factor of 2.

To illustrate the reduction of the Hamiltonian-matrix sizes through \mathcal{P}_1 symmetry, we indicate in Table VII the typical dimensions of the positive and negative parity blocks classi-

TABLE VII. Example of a reduction of the dimensions of the matrices to be diagonalized with the PSY-MB method, by making use of \mathcal{P}_1 and parity quantum numbers in a realistic case. The total number of basis configurations is 901 in this case.

\mathcal{P}_1 value	Dim. parity +	Dim. parity -
-4	4×4	5×5
-2	83×83	92×92
0	359×359	174×174
+2	83×83	91×91
+4	4×4	6×6

fied according to their \mathcal{P}_1 quantum numbers. Even though we could have easily diagonalized the matrices of the full cutoff (901×901 in the example), using \mathcal{P}_1 symmetry brings several smaller-size matrices and in addition offers the symmetry classification of the resulting solutions.

A. Empirical pairing strength determination

As it is well known from standard approaches such as the BCS approximation, the inclusion of a residual pairing interaction should be responsible for an important decrease of the nuclear moments of inertia.

In order to get an idea about the monopole-pairing strengths that one should consider optimal for our basis selection, we first consider the monopole pairing constants G_n and G_p taken from Ref. [26]:

$$\begin{cases} G_n = [19.30 - 0.084 (N - Z)]/A & \text{if } Z \geq 88, \\ G_n = [18.95 - 0.078 (N - Z)]/A & \text{if } Z < 88 \end{cases} \quad (4.1)$$

and

$$\begin{cases} G_p = [13.30 + 0.217 (N - Z)]/A & \text{if } Z \geq 88, \\ G_p = [17.90 + 0.176 (N - Z)]/A & \text{if } Z < 88. \end{cases} \quad (4.2)$$

Starting from the above expressions we have adjusted the multiplicative factor F necessary to bring the calculated val-

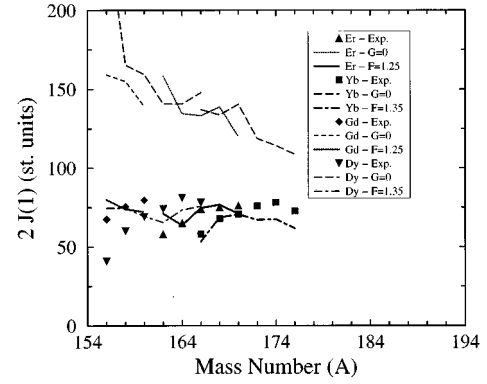


FIG. 9. Moments of inertia (standard units, \hbar^2/MeV) for the chains of Er, Yb, Gd, and Dy isotopes, and comparison to the experimental values. The plot also indicates the moments of inertia one would obtain in the case of zero pairing.

ues of the moments of inertia close to the experiment. The results are reported in Table VIII. From this table we can conclude that for the valence space of 20 particles on 40 levels and the many-particle cutoff configurations considered, the empirical multiplicative factor is $F \sim 1.30$.

B. Reduction of the moments of inertia for Er, Yb, Gd, and Dy isotopes

In order to illustrate the Fock space calculations, also when systematically varying Z and N numbers, we have performed calculations of the moments of inertia for the chains of isotopes of Er, Yb, Gd, and Dy nuclei. For these calculations, one central nucleus has been chosen in each chain, and the value of F has been adjusted for this nucleus. The obtained value of F has been kept constant for all the other isotopes of the same nuclide.

The results are plotted in Fig. 9 where we have indicated the experimental moments of inertia, and the calculated ones. In the same plot are also reported the results of the calculations one obtains when the residual pairing interaction is switched off.

TABLE VIII. Empirical determination of multiplicative factor F (common for protons and neutrons) adjusted to reproduce the experimentally observed moments of inertia of some selected nuclei in the rare-earth mass region. Columns (3) and (4) give the cranking spin values obtained at rotational frequency $\hbar\omega = 0.05$ MeV for protons and neutrons, respectively. These values have been used to calculate $J^{(1)} \equiv I/\omega$.

Nucleus	F	$\langle J_x \rangle_\pi^{\text{PSY-MB}}(\hbar)$	$\langle J_x \rangle_\nu^{\text{PSY-MB}}(\hbar)$	$2J_{\text{total}}^{(1)\text{PSY-MB}}(\hbar^2/\text{MeV})$	$2J_{\text{exp}}^{(1)}(\hbar^2/\text{MeV})$
^{158}Gd	0	1.214	2.660	154.96	75.5
^{158}Gd	1.25	0.525	1.323	73.92	75.5
^{160}Dy	0	1.173	2.811	159.36	69
^{160}Dy	1.35	0.556	1.179	69.40	69
^{168}Er	0	0.877	2.594	138.84	75
^{168}Er	1.25	0.462	1.457	76.76	75
^{170}Yb	0	0.810	2.701	140.44	71
^{170}Yb	1.35	0.459	1.303	70.48	71
^{186}W	0	0.466	1.555	80.84	48.5
^{186}W	1.35	0.275	0.986	50.44	48.5

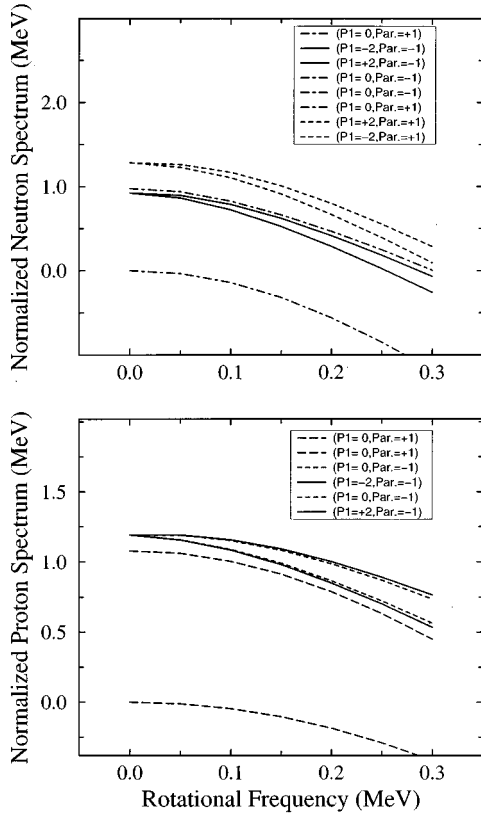


FIG. 10. Illustration of the phenomenon of \mathcal{P}_1 splitting in the calculated cranking spectra for neutrons (top) and protons (bottom) in the nucleus ^{168}Er ; for details see text and Ref. [18]. In both cases the spectra are normalized to the lowest eigenvalue obtained at zero rotational frequency.

We can see clearly from this figure that the calculated moments of inertia are consistent with the observed ones, giving therefore an indication that PSY-MB can be used in standard realistic situations. The characteristic small deviations from experiment when N varies have also been obtained in the standard BCS calculations, Ref. [26], and should *not* be attributed to the Fock space diagonalization method as its possible deficiency.

C. Illustration of the \mathcal{P} splitting on a realistic example

One of the interesting possibilities in the \mathcal{P} -symmetry context is that of comparison with the measured spectra. In fact, a possibility of finding an experimental evidence for \mathcal{P}_1 symmetry was already mentioned in Ref. [18]. The mechanism of \mathcal{P}_1 splitting consists in a splitting between the eigenvalues obtained for states with opposite \mathcal{P}_1 quantum numbers (that are degenerate at $\omega=0$), as the rotational frequency increases. One should not confuse the \mathcal{P} splitting with the well-known signature splitting phenomenon. In fact, the \mathcal{P} splitting corresponds to levels with opposite \mathcal{P}_1 but with the same signature quantum number [18].

In Fig. 10 we have reported the calculated many-body spectra obtained for the nucleus ^{168}Er for neutrons and protons. This figure shows that one obtains nonzero and measurable \mathcal{P}_1 splitting in the calculated many-body spectra. A difficulty is that \mathcal{P}_1 splitting requires, by definition, $\mathcal{P}_1 \neq 0$, $\mathcal{P}_1 = \pm 2$ being the first possibility. Corresponding states be-

long, when using the quasiparticle language, to configurations differing in terms of four QP's which corresponds to relatively high excitation energies—and thus a comparison of an experimental \mathcal{P}_1 splitting with theory requires a simultaneous measurement of two specific highly excited bands simultaneously—which seems to be not a totally trivial objective at present.

V. SUMMARY AND CONCLUSIONS

In this article we presented a many-body basis-optimization approach, called the PSY-MB (\mathcal{P} symmetry and many-body) method, adapted for treating the nuclear state-dependent pairing correlations in realistic calculations.

We have demonstrated that this method, based on a symmetry-oriented optimization of the many-body basis and of the basis cutoff, leads to reliable results both in model spaces and in realistic spaces. Advantages of this method lie in the fact that it conserves the number of particles and therefore does not show the known deficiencies, when the pairing interactions decrease, of particle nonconserving approaches such as the HFB formalism. On the contrary, the PSY-MB treatment becomes more reliable in the weak pairing limit.

Another advantage of the method is that it leads to a direct determination of many eigenvalues (within a given symmetry block) in a single diagonalization. Yet another advantage is the possibility of applying the same approach to the pairing Hamiltonians with nontrivially state dependent matrix elements. We have presented a simple model pairing interaction of a Gaussian type and illustrated a rapid stabilization of the obtained solutions with respect to a basis cutoff.

Finally we have demonstrated on the explicit examples with the realistic Woods-Saxon spectra that the seniority $s=0$ states compete very often with the two quasiparticle states, only the latter ones being usually treated within the BCS/HFB approaches; the PSY-MB method offers naturally a good description of these states.

ACKNOWLEDGMENTS

We would like to express our thanks to the *Institut de Développement et de Ressources en Informatique Scientifique* (IDRIS) of CNRS, France, for providing us with the computing facilities under Project No. 960333.

APPENDIX A: GENERAL \mathcal{P}_1 -SYMMETRIC HAMILTONIANS—AN ALTERNATIVE

As already mentioned in Sec. II, the most general \mathcal{P}_1 -symmetric Hamiltonian is represented by Eqs. (2.4), if the terms in Eqs. (2.4b) and (2.4e) vanish. Within a single-particle basis that obeys the $\hat{S}(1)$ symmetry we may write the one-body part of the Hamiltonian in the form

$$\begin{aligned} \sum_{\alpha\beta} \langle \alpha | \hat{h}(1) | \beta \rangle c_{\alpha}^{\dagger} c_{\beta} \rightarrow \sum_{\alpha^{+}} \sum_{\beta^{+}} \langle \alpha^{+} | \hat{h}(1) | \beta^{+} \rangle c_{\alpha^{+}}^{\dagger} c_{\beta^{+}} \\ + \sum_{\alpha^{-}} \sum_{\beta^{-}} \langle \alpha^{-} | \hat{h}(1) | \beta^{-} \rangle c_{\alpha^{-}}^{\dagger} c_{\beta^{-}}. \end{aligned} \quad (\text{A1})$$

It is now straightforward to observe [18] that by setting

$$\hat{g}_{\alpha+\beta+} \equiv c_{\alpha+}^\dagger c_{\beta+} \equiv \hat{N}_{\alpha+\beta+}, \quad (\text{A2a})$$

$$\hat{g}_{\alpha-\beta-} \equiv c_{\alpha-} c_{\beta-}^\dagger \equiv \hat{N}_{\alpha-\beta-}, \quad (\text{A2b})$$

$$\hat{g}_{\alpha+\beta-} \equiv c_{\alpha+}^\dagger c_{\beta-}^\dagger \equiv \hat{B}_{\alpha+\beta-}^+, \quad (\text{A2c})$$

$$\hat{g}_{\alpha-\beta+} \equiv c_{\alpha-} c_{\beta+} \equiv \hat{B}_{\alpha-\beta+}, \quad (\text{A2d})$$

we obtain an ensemble of operators satisfying the commutation rules

$$[\hat{g}_{kl}, \hat{g}_{pq}] = \delta_{lp} \hat{g}_{kq} - \delta_{kq} \hat{g}_{pl}; \quad k, l, p, q = 1, 2, \dots, n. \quad (\text{A3})$$

(In the last relation we introduced for convenience the indices numbering at the same time both classes of states, i.e., “ $\alpha+$ ” and “ $\alpha-$ ” within one uniform notation; the symbols \hat{N} , \hat{B} , and \hat{B}^+ will be needed below.)

The importance of relation (A3) lies in its representing the set of commutation relations that are characteristic for the generators of a unitary group in n dimensions $U(n)$. Denoting the generators of $U(n)$ by \hat{G}_{kl} , we can identify the two ensembles: $\{\hat{g}_{kl}\} \leftrightarrow \{\hat{G}_{kl}\}$. The Hamiltonian in question can be expressed in terms of the generators of the corresponding unitary group (see below) and the solutions of the eigenvalue problem transform according to the totally antisymmetric irreducible representations of $U(n)$. This observation allows us to apply any matrix representation of \hat{G}_{kl} known in the literature, such as, for instance, that of Gelfand and Zetlin [27], to obtain directly a many-body matrix representation of the Hamiltonians in question. One can show that the related Hamiltonian, composed of the one-body (A1) and the two-body term (2.4) [where Eqs. (2.4b)–(2.4e) have been excluded], written down in the many-body representation is [compare with Eq. (A2)]

$$\begin{aligned} \hat{H} = & A_0 + \sum_{\alpha+\beta+} A_1^+ \hat{N}_{\alpha+\beta+} + \sum_{\alpha-\beta-} A_1^- \hat{N}_{\alpha-\beta-} \\ & + \sum_{\substack{\alpha+\beta+ \\ \gamma+\delta+}} A_2^+ \hat{N}_{\alpha+\beta+} \hat{N}_{\gamma+\delta+} + \sum_{\substack{\alpha-\beta- \\ \gamma-\delta-}} A_2^- \hat{N}_{\alpha-\beta-} \hat{N}_{\gamma-\delta-} \\ & + \sum_{\substack{\alpha+\beta- \\ \gamma-\delta+}} A_3 \hat{B}_{\alpha+\beta-}^+ \hat{B}_{\gamma-\delta+}, \end{aligned} \quad (\text{A4})$$

where

$$\begin{aligned} A_0 = & \sum_{\alpha-} \langle \alpha- | \hat{h}(1) | \alpha- \rangle \\ & + \frac{1}{2} \sum_{\alpha-\beta-} \langle \alpha-\beta- | \widetilde{\hat{h}(2)} | \alpha-\beta- \rangle, \end{aligned} \quad (\text{A5a})$$

$$A_1^+ = \langle \alpha+ | \hat{h}(1) | \beta+ \rangle + \frac{1}{2} \sum_{\gamma+} \langle \alpha+\gamma+ | \hat{h}(2) | \beta+\gamma+ \rangle, \quad (\text{A5b})$$

$$\begin{aligned} A_1^- = & -\langle \beta- | \hat{h}(1) | \alpha- \rangle + \sum_{\gamma-} \langle \beta-\gamma- | \hat{h}(2) | \gamma-\alpha- \rangle \\ & - \frac{1}{2} \sum_{\gamma-} \langle \beta-\gamma- | \hat{h}(2) | \alpha-\gamma- \rangle, \end{aligned} \quad (\text{A5c})$$

$$A_2^+ = -\frac{1}{2} \langle \alpha+\gamma+ | \hat{h}(2) | \delta+\beta+ \rangle, \quad (\text{A5d})$$

$$A_2^- = -\frac{1}{2} \langle \beta-\delta- | \hat{h}(2) | \gamma-\alpha- \rangle, \quad (\text{A5e})$$

$$A_3 = \langle \alpha+\beta- | \widetilde{\hat{h}(2)} | \delta+\gamma- \rangle. \quad (\text{A5f})$$

For p particles on n levels, the corresponding dimension of the \hat{G}_{kl} matrices $[\hat{G}_{kl}]_{ij}$ is given by the Newton symbol $\dim(n, p) \equiv \binom{p}{n}$; $i, j = 1, 2, \dots, \dim(n, p)$ (compare Sec. II B). The first order Casimir operator can be constructed:

$$\begin{aligned} \hat{C} \equiv & \sum_k^n \hat{g}_{kk} = \sum_{\alpha+}^{N_+} \hat{g}_{\alpha+\alpha+} + \sum_{\alpha-}^{N_-} \hat{g}_{\alpha-\alpha-} \\ = & \sum_{\alpha+}^{N_+} c_{\alpha+}^\dagger c_{\alpha+} + \sum_{\alpha-}^{N_-} c_{\alpha-} c_{\alpha-}^\dagger \\ = & \hat{\mathcal{N}}_1^+ - \hat{\mathcal{N}}_1^- + N_-, \end{aligned} \quad (\text{A6})$$

where the auxiliary operators

$$\hat{\mathcal{N}}_1^+ \equiv \sum_{\alpha+}^{N_+} c_{\alpha+}^\dagger c_{\alpha+}$$

and

$$\hat{\mathcal{N}}_1^- \equiv \sum_{\alpha-}^{N_-} c_{\alpha-} c_{\alpha-}^\dagger, \quad (\text{A7})$$

give the number of particles with symmetry $+$ and $-$, respectively. This Casimir operator is obviously a symmetry operator for the Hamiltonian since $[\hat{C}, \hat{g}_{ik}] = 0 \quad \forall i, k$, so that we have

$$[\hat{H}, \hat{C}] = 0 \leftrightarrow [\hat{H}, (\hat{\mathcal{N}}_1^+ - \hat{\mathcal{N}}_1^-)] = 0. \quad (\text{A8})$$

Defining

$$\hat{\mathcal{P}}_1 \equiv (\hat{\mathcal{N}}_1^+ - \hat{\mathcal{N}}_1^- + N_-) - N_- = \hat{\mathcal{N}}_1^+ - \hat{\mathcal{N}}_1^-, \quad (\text{A9})$$

i.e., arbitrarily normalizing the $\hat{\mathcal{P}}_1$ operator in order to get rid of the additive constant in Eq. (A6), we find that all the solutions can be numbered with the quantum number \mathcal{P}_1 , an eigenvalue of the $\hat{\mathcal{P}}_1$ operator and that the corresponding quantum numbers take the values (2.16) and (2.17) indicated in Sec. II B. In this case the number \mathcal{P}_1 represents again the

difference between the number of particles occupying the states ($s_\alpha = +i$) and the number of particles occupying the states ($s_\alpha = -i$).

The results of the above discussion can easily be extended to the case of the Hamiltonians whose two-body terms are generalized to include, e.g., the quadratic forms in terms of *all* the generators (A2). Such Hamiltonians may contain terms of the following structure:

$$\hat{B}_{\alpha+\beta}^+ \hat{B}_{\gamma+\delta}^+ \rightarrow (\text{two-pair creation, } \Delta n = 4), \quad (\text{A10a})$$

$$\hat{B}_{\alpha-\beta} \hat{B}_{\gamma-\delta} \rightarrow (\text{two-pair annihilation, } \Delta n = -4), \quad (\text{A10b})$$

$$\hat{B}_{\alpha+\beta}^+ \hat{B}_{\gamma-\delta} \rightarrow (\text{one-pair scattering, } \Delta n = 0), \quad (\text{A10c})$$

$$\begin{aligned} \hat{B}_{\alpha+\beta}^+ \hat{N}_{\gamma+\delta} &\rightarrow (\text{one-pair creation,} \\ &\text{one-particle scattering, } \Delta n = 2), \end{aligned} \quad (\text{A10d})$$

$$\begin{aligned} \hat{B}_{\alpha+\beta}^+ \hat{N}_{\gamma-\delta} &\rightarrow (\text{one-pair creation,} \\ &\text{one-particle scattering, } \Delta n = 2), \end{aligned} \quad (\text{A10e})$$

$$\hat{B}_{\alpha-\beta} \hat{N}_{\gamma+\delta} \rightarrow (\text{one-pair annihilation,}$$

$$\text{one-particle scattering, } \Delta n = -2), \quad (\text{A10f})$$

$$\begin{aligned} \hat{B}_{\alpha-\beta} \hat{N}_{\gamma-\delta} &\rightarrow (\text{one-pair annihilation,} \\ &\text{one-particle scattering, } \Delta n = -2). \end{aligned} \quad (\text{A10g})$$

In the above expression an interpretation in terms of the physical significance of the contributing matrix elements as well as the fact of nonconservation of the number of particles ($\Delta n = \pm 4, \Delta n = \pm 2$) by the generalized form of the Hamiltonian have been indicated.

The Casimir operator (A6) still commutes with such a generalized Hamiltonian and consequently

$$\hat{\mathcal{P}}_1 = \hat{\mathcal{N}}_1^+ - \hat{\mathcal{N}}_1^- \quad (\text{A11})$$

is a symmetry operation of that more general Hamiltonian as well. Hamiltonians of that mathematical form can be studied in particular in the context of Bogolyubov transformations. Here we do not examine their properties further since the principal goal of this work is to study the particle-number conserving algorithms. These Hamiltonians are also of interest within the models that explicitly allow a variation of the particle numbers.

Let us emphasize that in the case examined here the $\hat{\mathcal{N}}_1^+ + \hat{\mathcal{N}}_1^-$ operator has no interest since it does not commute with the Hamiltonian. This example demonstrates also the advantage of the formulation in terms of the \mathcal{P} -symmetry language ($\hat{\mathcal{P}}_1 \equiv \hat{\mathcal{N}}_1^+ - \hat{\mathcal{N}}_1^-$) and that this is the only possible formulation of the related symmetry problem in this case.

-
- [1] R.W. Richardson, Phys. Rev. **141**, 949 (1966).
[2] C.S. Wu and J.Y. Zeng, Phys. Rev. C **39**, 666 (1989).
[3] J.Y. Zeng and T.S. Cheng, Nucl. Phys. **A405**, 1 (1983).
[4] J.Y. Zeng, T.S. Cheng, L. Cheng, and C.S. Wu, Nucl. Phys. **A411**, 49 (1983).
[5] J.Y. Zeng, T.S. Cheng, L. Cheng, and C.S. Wu, Nucl. Phys. **A414**, 253 (1984).
[6] J.Y. Zeng, T.S. Cheng, L. Cheng, and C.S. Wu, Nucl. Phys. **A421**, 125c (1984).
[7] L. Lin, Phys. Rev. C **51**, 3017 (1995).
[8] J.Y. Zeng, Y.A. Lei, T.H. Jin, and Z.J. Zhao, Phys. Rev. C **50**, 746 (1994).
[9] J.Y. Zeng, T.H. Jin, and Z.J. Zhao, Phys. Rev. C **50**, 1388 (1994).
[10] J.Y. Zeng, C.S. Wu, L. Cheng, and C.Z. Lin, Phys. Rev. C **41**, 2911 (1990).
[11] J.A. Sheikh, M.A. Nagarajan, N. Rowley, and K.F. Pal, Phys. Lett. B **223**, 1 (1989).
[12] J.A. Sheikh, N. Rowley, and M.A. Nagarajan, Phys. Rev. C **42**, 787 (1990).
[13] C.S. Wu and J.Y. Zeng, Phys. Rev. C **40**, 998 (1989).
[14] C.S. Wu and J.Y. Zeng, Phys. Rev. C **41**, 1822 (1990).
[15] C.S. Wu and J.Y. Zeng, Phys. Rev. Lett. **66**, 1022 (1991).
[16] C.S. Wu and J.Y. Zeng, Phys. Rev. C **44**, 2566 (1991).
[17] L.I. Schiff, *Quantum Mechanics* (McGraw-Hill, New York, 1968), p. 227.
[18] O. Burglin, J. Dudek, B. Heydon, N. El-Aouad, N. Rowley, W. Satula, and Z. Szymański, Phys. Rev. C **51**, 547 (1995).
[19] M. Moshinsky, *Group Theory and the Many-Body Problem* (Gordon and Breach, New York, 1968).
[20] O. Burglin and N. Rowley, Nucl. Phys. **A602**, 21 (1996).
[21] T.R. Werner and J. Dudek, At. Data Nucl. Data Tables **59**, 1 (1995).
[22] M. Hasegawa and S. Tazaki, Phys. Rev. C **35**, 1508 (1987).
[23] R.W. Richardson, J. Math. Phys. (N.Y.) **6**, 1034 (1965).
[24] R.W. Richardson, Phys. Lett. **14**, 325 (1965).
[25] J. Dudek, J. Phys. C **10**, 18 (1980).
[26] J. Dudek, A. Majhofer, and J. Skalski, J. Phys. G **6**, 447 (1980).
[27] I.M. Gelfand and M.L. Zetlin, Dokl. Akad. Nauk SSSR **71**, 825 (1950); **71**, 1017 (1950).